Electronic Supplementary Material (ESI) for Organic & Biomolecular Chemistry.

Supporting Information: Selective Photoredox Direct Arylations of Aryl Bromides in Water in Microfluidic Reactor

Francesca Pallini,[†] Elena Sangalli,[†] Mauro Sassi,[‡] Philippe M. C. Roth,[¶] Sara Mattiello,[*,‡] and Luca Beverina[*,‡]

[†]*Department of Materials Science, University of Milano-Bicocca, Via R. Cozzi 55, I-20125 Milano, Italy*

[‡]*Department of Materials Science, University of Milano-Bicocca and INSTM, Via R. Cozzi, 55, Milano, Italy. I-20125*

[¶]*Corning SAS Reactor Technologies, 7 bis Avenue de Valvins CS 70156 Samois-sur-Seine, F-77210 AVON Cedex, France. E-mail: reactors@corning.com*

E-mail: sara.mattiello@unimib.it; luca.beverina@unimib.it

Contents

1 Information on optical and electrochemical characterizations

DLS experiments were performed on a 90Plus particle size analyzer (Brookhaven Instruments Corp.) equipped with a 35 mW solid state 632.8 nm laser.

Absorption spectra were collected with a Jasco V-570 spectrophotometer, while PL spectra were collected with a Varian Cary Eclipse spectrofluorometer. Unless when otherwise stated, experiments were performed in a quartz cuvette (optical pathway 10 mm).

Electrochemical analysis was performed with an EG&G Princeton Applied 2273 potentiostat/galvanostat in glove box in a three-electrode glass cell using a glassy carbon pin as working electrode (diameter of 2 mm), a platinum mesh as counter electrode, and Ag/AgCl wire as the quasi-reference electrode at 50 mV/s scanning speed.

2 Details on photochemical setup

2.1 Photochemical setup for reactions in batch

Reactions were performed in a cylindrical 10 mL vial (~1.35 cm diameter). Reactions were irradiated with a set of four 9 W UV-A lamps (λ_{max}= 365 nm) and kept under magnetic stirring. A flow of compressed air was used to maintain the reactions at room temperature. Figure S1 shows the photochemical setup.

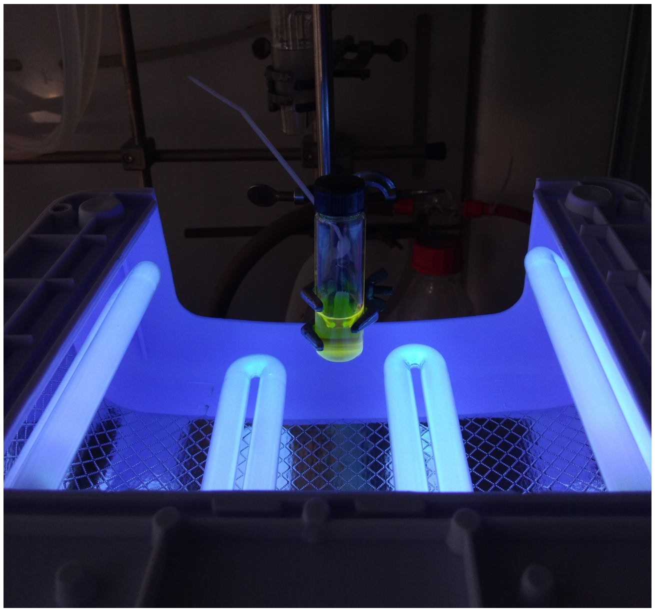

Figure S1 Picture of the photochemical setup used for batch reactions

2.2 Corning® Lab Photo Reactor

The Corning ® Lab Photo Reactor is a glass-made microfluidic reactor characterized by channels width of 400 µm. This photoreactor is provided of a set of LED lamps centered around different wavelengths. LED and reactor temperature are controlled through two separate heating circulators. A pump injects the reaction mixture within the reactor at a controlled flow rate, and the mixture comes out from the outlet tubing. If allowed to pour in the inlet vessel, the reaction mixture can be easily recirculated. The main features of this reactor are shown in figure S2

All reactions were performed under the same working conditions (optimization of reactions parameter is discussed in Section 8). A 365 nm LED light was selected as irradiation source and was used at 70% of maximum intensity (radiant flux: 30.5 W); LED temperature was kept at 20 °C; flow rate inside the reactor was set to 8 mL/min and the reactor temperature was fixed to 25 °C. The reaction mixture was recirculated and tubings were coated with aluminum foil to avoid photocatalyst activation under the environmental light. The flask was kept within a secondary container, coated with aluminum foil as well. Due to recirculation, only 1/5 of the reaction volume could be illuminated at any given time, so the actual irradiation time is considered as 1/5 of the overall reaction time.

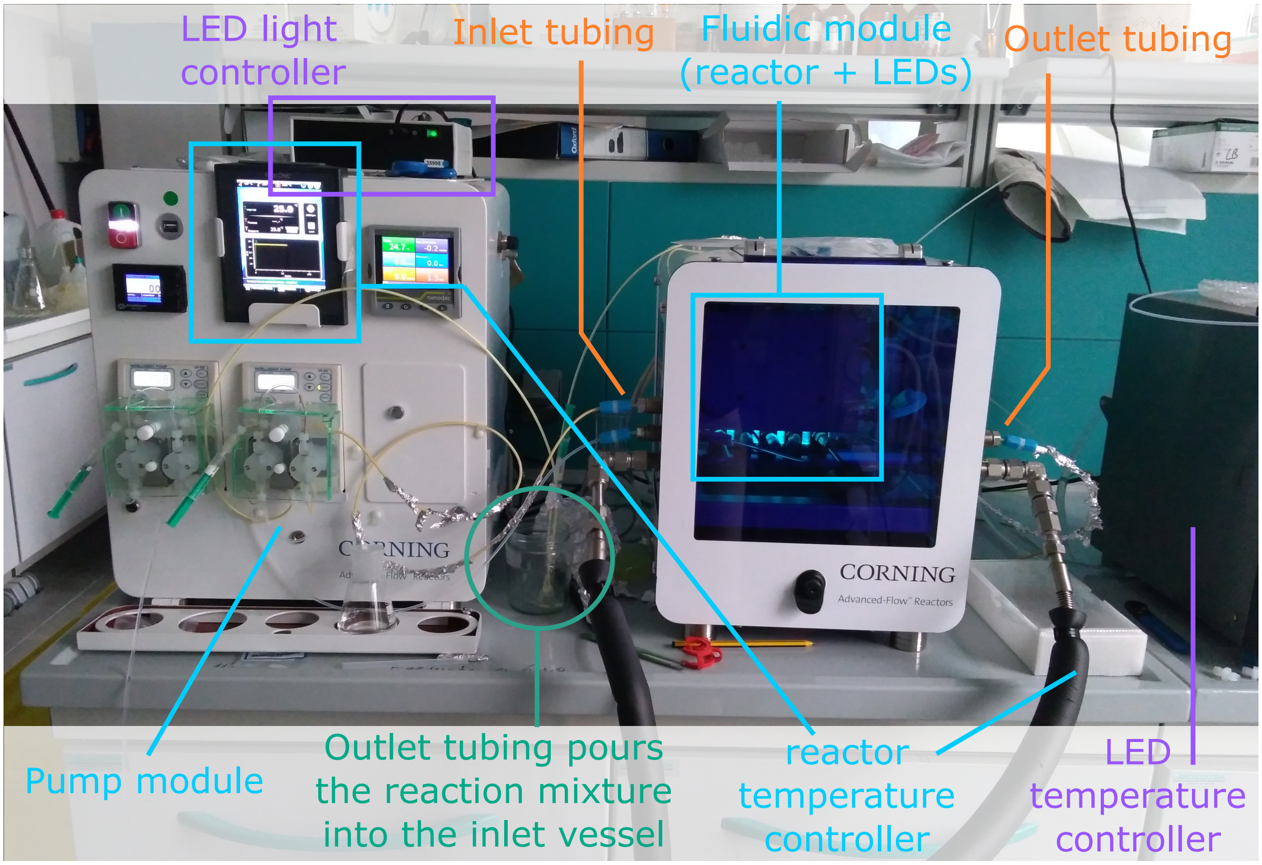

Figure S2 The Corning® Lab Photo Reactor

2.3 Chemtrix Labtrix® Start flow system

The Chemtrix Labtrix® Start is a continuous flow reactor system with modular design, which includes a syringe pump and a reactor module equipped with a Peltier device for temperature control. The main features of this reactor are shown in figure S3A. We operated it with the Labtrix 3223 glass reactor, characterized by channels width of 300 µm, and thickness of 120 µm, and inner volume of 10 µL (see Figure S3B, and Figure S10C). As the light source, we used a set of four 9 W UV-A lamps (λ_{max}= 365 nm), the same ones used for batch reactions. Figure S3C shows the reactor working under illumination.

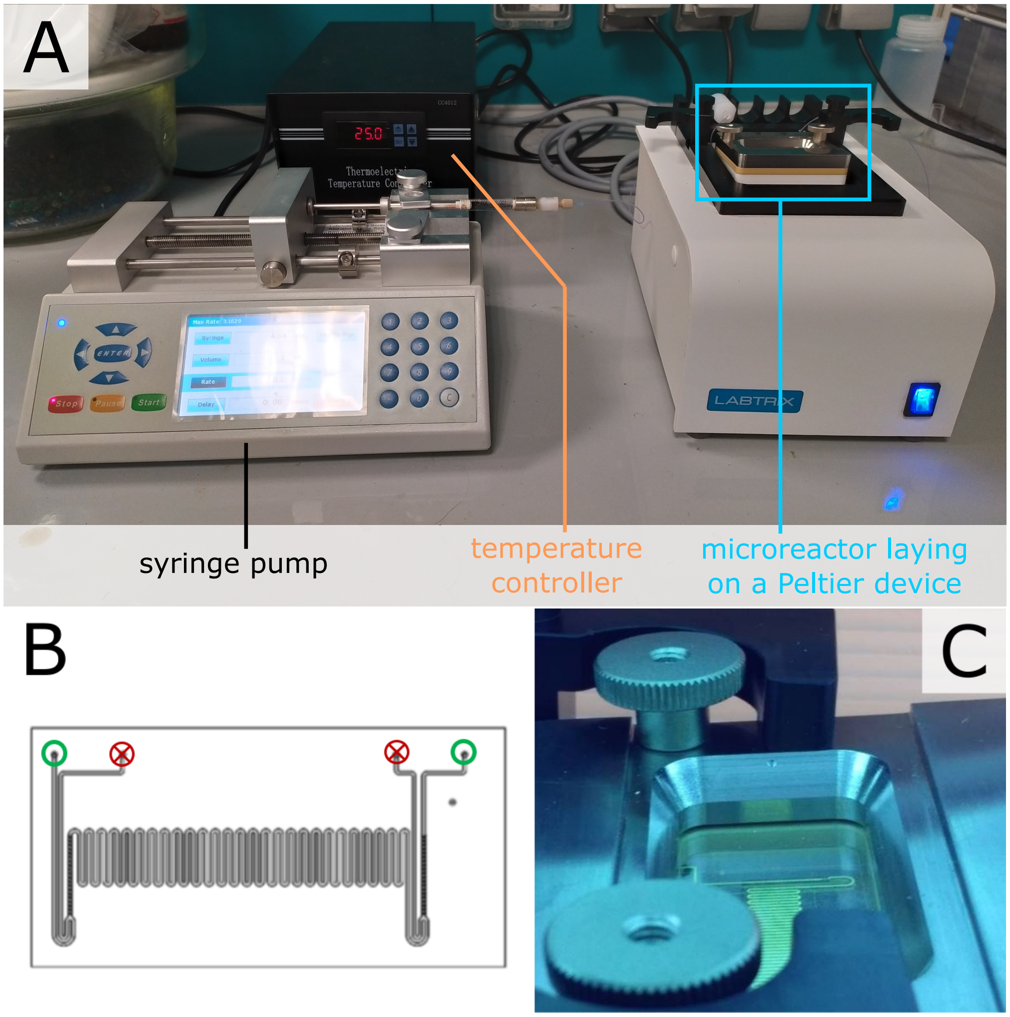

Figure S3 A) Picture of the Chemtrix Labtrix® Start flow reactor system. B) Graphical representation of the Chemtrix 3223 reactor. Inlet and outlet are highlighted in green circles, while the secondary inlet and outlet (red crosses) were kept closed. C) Picture of the reactor working under illumination.

The reaction mixture is injected within the microreactor at a $0.1\,\mu\mathrm{L\,min^{-1}}$ flow rate, thus remaining under illumination for 100 minutes. As the reaction mixture is injected with a syringe, this system does not allow for reaction mixture recirculation.

2.4 Evaluation of the irradiance of the light sources

Irradiance (365 nm wavelength) of the UV sources was evaluated through a THORLABs S120VC - Standard Photodiode Power Sensor, Si UV extended, wavelength range: 200 - 1100 nm, power range 50 nW-50 mW.

Lamps were switched on several minutes before starting measurements in order to reach regime conditions. The photodiode sensor was positioned at the same distance from the lamps as the reaction vessel/channels (3.5 cm in the case of the Corning® Lab Photo Reactor, 8 cm in the case of the Chemtrix Labtrix® Start and for batch reactions). Irradiation intensity data were acquired over two consecutive minutes every ten seconds.

Averaging each set of measurements and considering a 5% instrumental error, the irradiance of the UV-A lamp used for reactions in batch and with the Chemtrix Labtrix® Start was evaluated as $2.0{\pm}0.1\,\mathrm{mW\,cm^{-2}}$, while the irradiance of the LEDs of the Corning® Lab Photo Reactor was evaluated as $30.0{\pm}1.5\,\mathrm{mW\,cm^{-2}}$ (at 70% power intensity and for one LED panel only).

3 E-factor for the synthesis of photocatalysts

3.1 E-factor for the synthesis of PTh-OMe

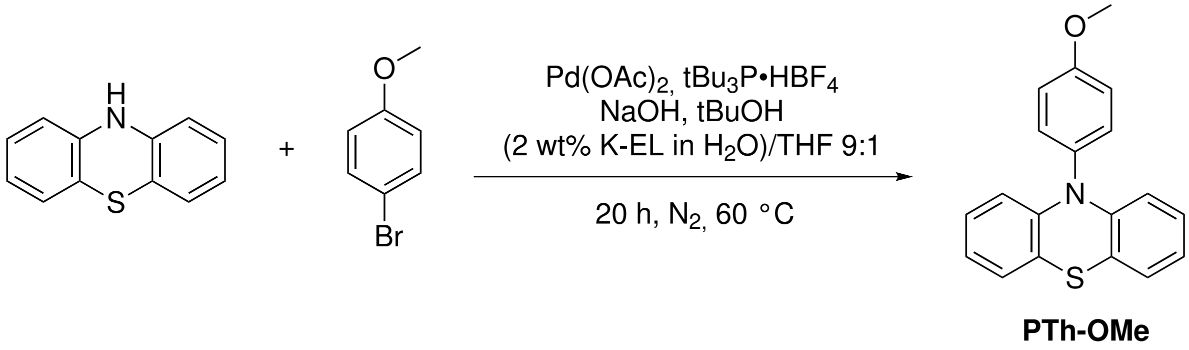

Chemical	Weight reagent (g)	Weight solvent (g)	Weight workup (g)
Phenothiazine	10.000		
4-bromoanisole	9.740		
NaOH	3.015		
$Pd(OAc)_2$	0.226		
$(^tBu)_3PHBF_4$	0.587		
^{t}BuOH	5.590		
Kolliphor ELP	0.912		
Water		45.000	20.000
THF		4.445	
EtOH			118.35
AcOEt			198.44
PTh-OMe product		12.550 g	

Water was included in the E-factor calculation, as it can be contaminated by palladium, and must therefore be treated as an hazardous waste.

The following densities were used to calculate the mass of employed solvents:

THF: $0.889\,\mathrm{g\,mL^{-1}}$; EtOH: $0.789\,\mathrm{g\,mL^{-1}}$; AcOEt: $0.902\,\mathrm{g\,mL^{-1}}$.

$$\text{E-factor}=\frac{\text{mass of reagents}+\text{mass of solvents}+\text{mass of workup - mass of product}}{\text{mass of product}}=$$

$$=\frac{30.070\,\mathrm{g}+49.445\,\mathrm{g}+336.790\,\mathrm{g}-12.550\,\mathrm{g}}{12.550\,\mathrm{g}}=32.17$$

3.2 E-factor for the synthesis of S-PTh

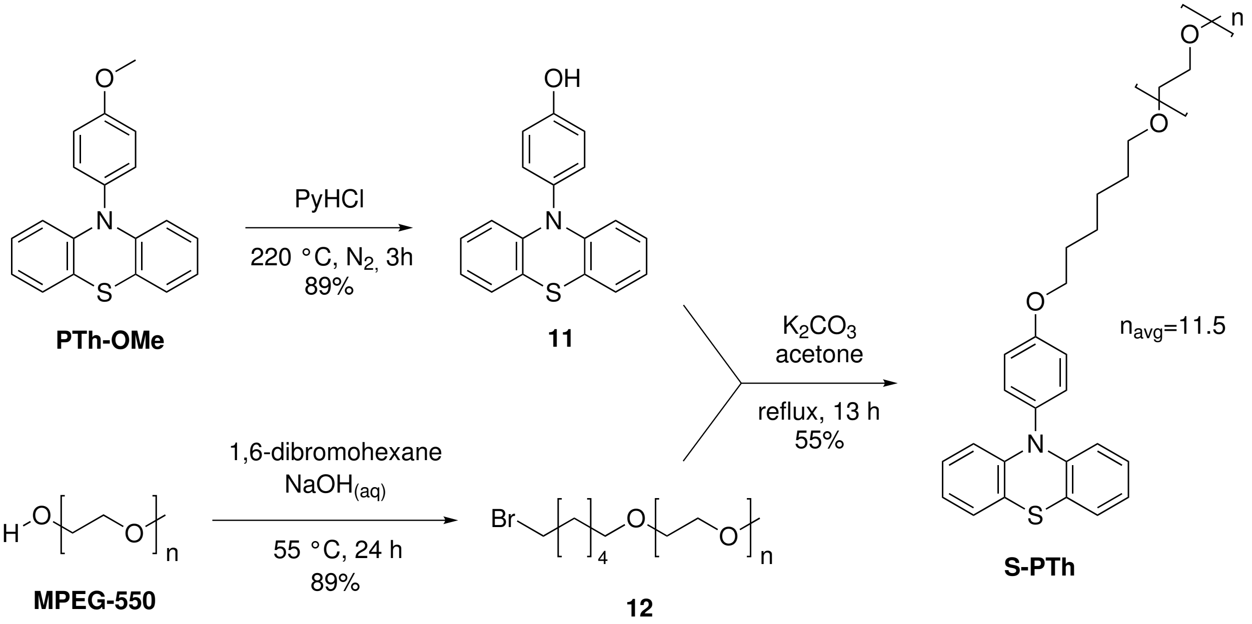

Scheme S1 Synthetic route to **S-PTh** from **PTh-OMe**, 1,6-dibromohexane and **MPEG-550**.

S-PTh was synthesized with a 3 step procedure summarized in Scheme S1. Details on each synthetic step are reported subsequently.

3.2.1 Derivative 11

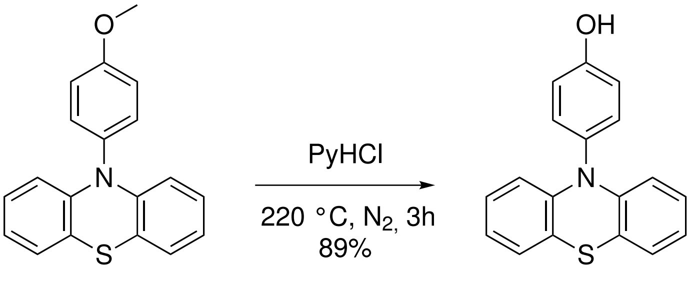

PTh-OMe

11

Chemical	Weight reagent (g)	Weight solvent (g)	Weight workup (g)
PTh-OMe	7.000		
PyHCl	26.480		
$NaHSO_3$			1.600
Water			78.400
Product 11		6.000 g	

$$\text{E-factor}=\frac{\text{mass of reagents}+\text{mass of workup - mass of product}}{\text{mass of product}}=$$

$$=\frac{33.480\,\text{g}+80.000\,\text{g}-6.000\,\text{g}}{6.000\,\text{g}}=17.91$$

3.2.2 Derivative 12

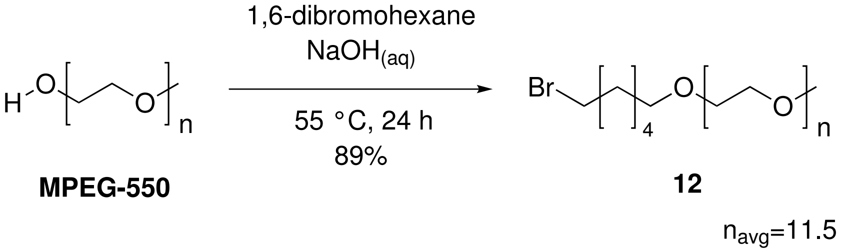

Chemical	Weight reagent (g)	Weight solvent (g)	Weight workup (g)
MPEG-550	30.000		
1,6-dibromohexane	66.500		
Et_2O			21.390
AcOEt			45.10
Product 12		34.770 g	

Water and inorganic salts were excluded from the the E-factor calculation, as the aqueous phase was always recovered by phase separation, and it could be contaminated only by salts and M-PEG (which is non-toxic and non-hazardous). The following densities were used to calculate the mass of employed solvents:

Et_2O: $0.713\,\mathrm{g\,mL^{-1}}$; AcOEt: $0.902\,\mathrm{g\,mL^{-1}}$.

$$\text{E-factor}=\frac{\text{mass of reagents} + \text{mass of workup - mass of product}}{\text{mass of product}}=$$

$$=\frac{96.500\,\mathrm{g} + 66.490\,\mathrm{g} - 34.770\,\mathrm{g}}{34.770\,\mathrm{g}}=3.69$$

3.2.3 S-PTh

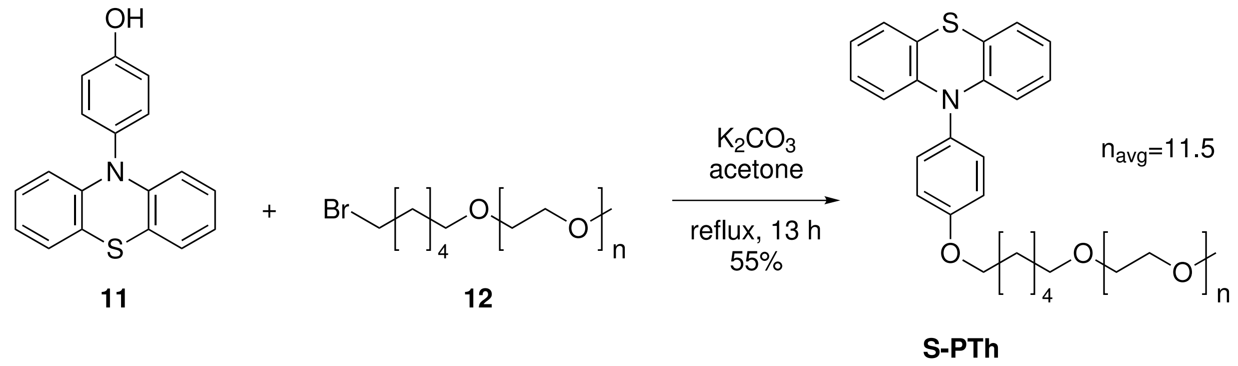

Chemical	Weight reagent (g)	Weight solvent (g)	Weight workup (g)
Derivative 11	2.430		
Derivative 12	6.000		
K_2CO_3	1.730		
Acetone		7.840	7.840
Silica			8.000
Product S-PTh		4.158 g	

Acetone density used in the calculation: $0.784\,\mathrm{g\,mL^{-1}}$.

Solvents used for Soxhlet extraction are not included in the E-factor calculation, as they were recovered by distillation ad the end of the process.

$$\text{E-factor}=\frac{\text{mass of reagents}+\text{mass of solvents}+\text{mass of workup - mass of product}}{\text{mass of product}}=$$

$$=\frac{10.160\,\mathrm{g}+7.840\,\mathrm{g}+15.840\,\mathrm{g}-4.158\,\mathrm{g}}{4.158\,\mathrm{g}}=7.14$$

3.2.4 Overall E-factor for the synthesis of S-PTh

To synthesize 1 g of **S-PTh**, 0.584 g of derivative **11** and 1.443 g of derivative **12** are necessary, and 7.14 g of waste are produced.

To synthesize 1.443 g of derivative **12**, 5.32 g of waste are produced.

To synthesize 0.584 g of derivative **11**, 0.681 of **PTh-OMe** are necessary 10.46 g of waste are produced.

To synthesize 0.681 of **PTh-OMe**, 21.9 g of waste are produced.

The overall E-factor for the synthesis of **S-PTh** is therefore

$$\text{E-factor}=7.36+5.32+10.46+21.9=44.8$$

4 PTh-OMe optical and electrochemical characterization

4.1 PTh-OMe absorption/PL spectra and CV

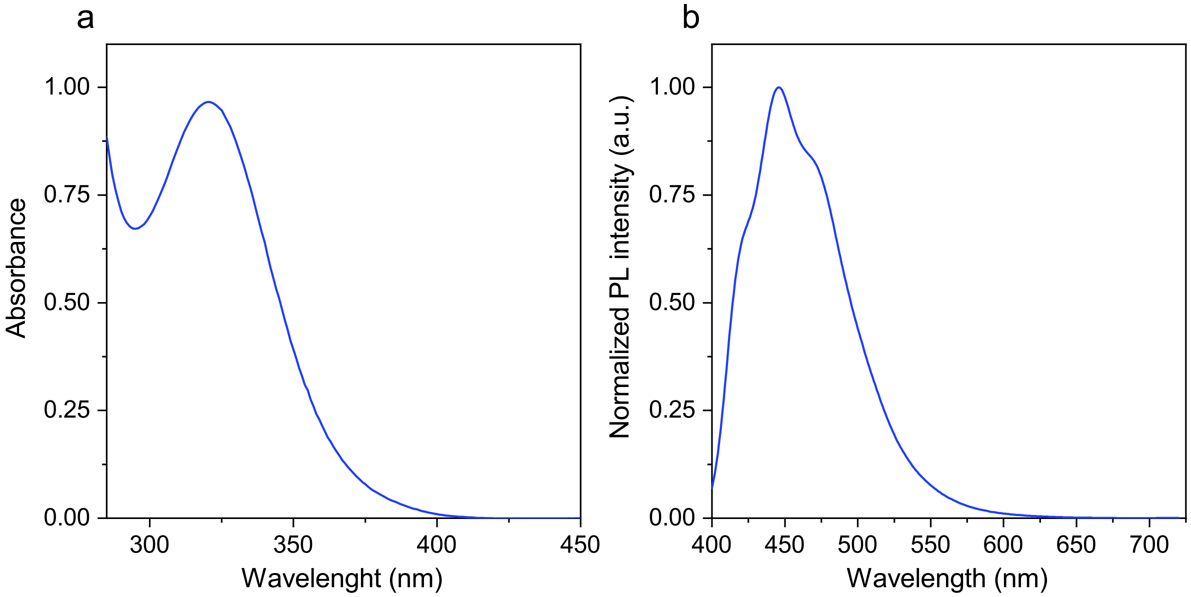

Figure S4 a) absorption and b) normalized PL spectrum of a 0.25 mM solution of **PTh-OMe** in acetonitrile. PL spectrum was collected using an excitation wavelength of 380 nm.

Figure (S4) shows absorption and PL spectra of **PTh-OMe** in acetonitrile. The photocatalyst absorption maximum lies around 320 nm, while the fluorescence maximum is around 445 nm, consistent with values reported in the literature.[S1][S2] Molar extinction coefficient was evaluated by least square method on a set of four solutions at different concentration of **PTh-OMe**, obtaining

$$\varepsilon(\lambda\text{=320nm}) = 3970 \pm 20\ \mathrm{M^{-1}cm^{-1}}$$

and

$$\varepsilon(\lambda\text{=365nm}) = 660 \pm 10\ \mathrm{M^{-1}cm^{-1}}$$

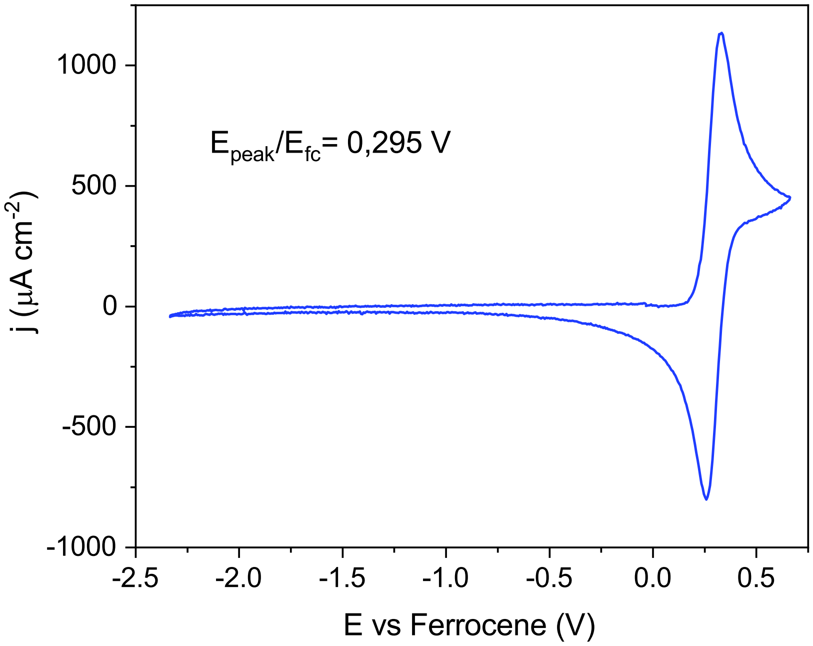

Figure S5 CV of a 5 mM solution of **PTh-OMe** in acetonitrile. Tetrabutylammonium hexafluorophosphate 0.1 M was used as the electrolyte, and a 0.001 M solution of ferrocene was used for calibration.

Figure S5 shows the cyclic voltammetry of a 5 mM **PTh-OMe** solution in acetonitrile. The measurement was collected at room temperature under inert atmosphere and potential values are reported against ferrocene. Oxidation potential of **PTh-OMe** was estimated from the half sum of anodic and cathodic peak potentials as 0.295 V vs ferrocene, corresponding to 0.675 V vs SCE (ferrocene potential against Saturated Calomel Electrode is 0.380 V in acetonitrile at room temperature).[S3]

4.2 Evaluation of PTh-OMe photoreduction potential

Photoreducing potential of the catalyst (cat) excited state can be evaluated through the equation[S4]

$$\mathrm{E_{ox}}^{*}(\mathrm{cat}^{\bullet+}/\mathrm{cat}^{*})=\mathrm{E_{ox}}(\mathrm{cat}^{\bullet+}/\mathrm{cat})-\mathrm{E_{0\text{-}0}}$$

where $\mathrm{E_{ox}}(\mathrm{cat}^{\bullet+}/\mathrm{cat}^{*})$ is the oxidation potential of the photocatalyst ground state and $\mathrm{E_{0\text{-}0}}$ is the energy of the compound excited state.

As reported in the literature,[S1,S5] $\mathrm{E_{0\text{-}0}}$ can be evaluated from the fluorescence spectrum (see figure S4b) using equation

$$\mathrm{E_{0\text{-}0}} = \mathrm{hc}/\lambda_{\mathrm{max}}$$

where h is the Planck constant (expressed in $\mathrm{eV \cdot s}$), c is the speed of light in vacuum (expressed in nm/s) and λ_{max} the fluorescence maximum (445 nm). A value of 2.79 eV was obtained for **PTh-OMe** (a conversion factor of 1 eV/V was considered to express such value in V).

Using this value and the oxidation potential obtained from CV, the **PTh-OMe** excited state reducing potential can be evaluated as -2.11±0.01 V vs SCE. The value results comparable with that reported for the well-known 10-phenylphenothiazine photocatalyst (-2.1 V vs SCE in acetonitrile),[S5] and close to those calculated for **PTh-OMe** in other solvents (e.g. -1.99 in DMA, where 10-phenylphenothiazine photoredox potential is evaluated to be -1.97 V vs SCE).[S1]

5 DLS characterization of S-PTh with and without K-EL

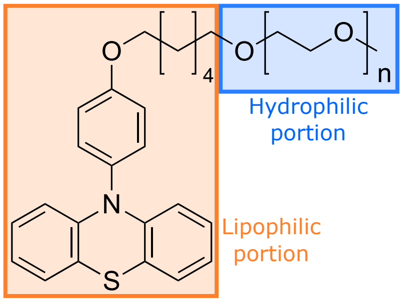

S-PTh was designed to display a surfactant behaviour, as it features both a lipophilic and a hydrophilic portion (here highlighted in orange and blue color respectively) covalently linked.

The DLS analysis of an aqueous solution of **S-PTh** (Figure S6) clearly shows the presence of aggregates in water, specifically two different families are present, having average diameters of ∼9 nm and ∼200 nm. This behavior is compatible with a micellization process.

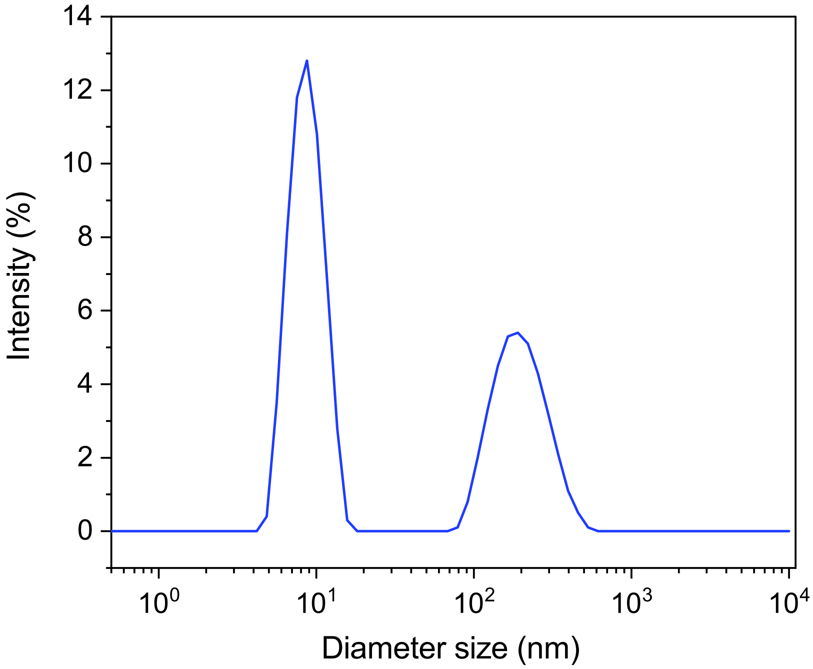

	Peak maximum	Integrated intensity
Peak 1	8.7 nm	60.2%
Peak 2	207 nm	39.8%

Figure S6 DLS analysis of a 2 wt% aqueous solution of **S-PTh**.

When **S-PTh** is mixed with K-EL (**S-PTh**/K-EL ratio: ~83/100 w/w), the DLS analysis detects only one family of particles (see Figure S7). The average dimension of such particles is comparable with that observed for K-EL alone. The disappearance of the family of larger aggregates suggests that **S-PTh** can effectively mix with K-EL, forming a pseudophase of mixed surfactants micelles.

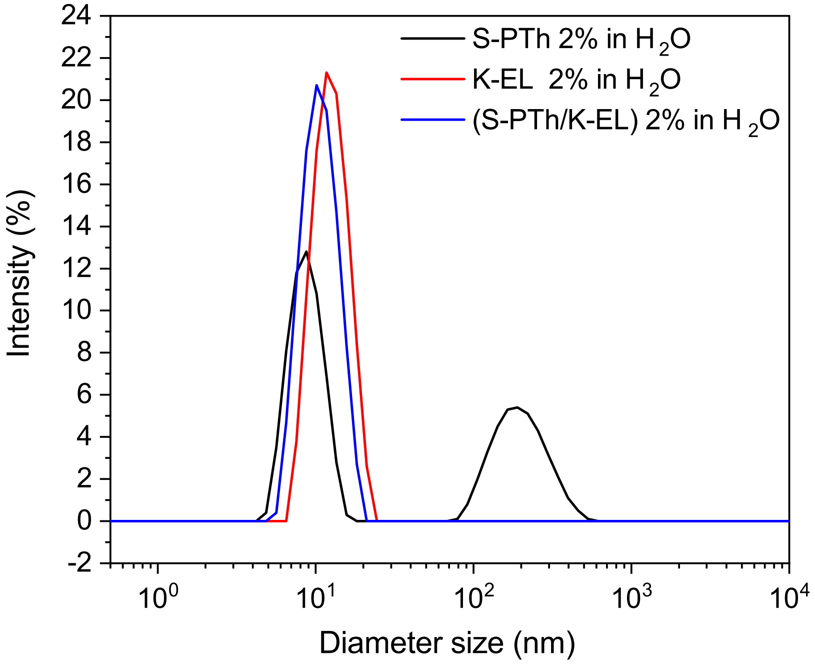

	S-PTh (Peak 1)	K-EL	S-PTh/K-EL mixture
Diameter size @maximum intensity	8.7 nm	11.7 nm	10.1 nm

Figure S7 Comparison between the DLS analysis of a 2 wt% aqueous solution of **S-PTh** (black line), a 2 wt% aqueous solution of K-EL (red line), and 2 wt% aqueous solution of a **S-PTh**/K-EL mixture (~83/100 w/w, blue line).

6 Emulsions stability as function of the surfactant

The choice of the surfactant to employ in this study was dictated by the need for a stable formulation state for the whole duration of the reaction. Reactions in emulsion, in fact, might suffer from reproducibility issues, and the capability of the surfactant to maintain a stable emulsion is fundamental to avoid phase segregation.[S6] This aspect is particularly important in this work, as some of the described couplings required reaction times in the order of days when performed in batch. Moreover, in the case of reactions performed with the Chemtrix Labtrix® Start system, the emulsion remains within the syringe for 1-7 days before it passes through the microfluidic reactor. It is therefore mandatory for the emulsion to remain stable for this whole time, even without stirring or mixing.*

As the surfactants, we tested K-EL, Tween 80 (T80), Brij L-23 (BL23), Triton X-100 (TX100) and TPGS-750-M (TPGS). Neutral surfactants only where taken in consideration, as ionic surfactants can interfere with the catalytic cycle and the reaction outcome. As the reaction, we chose the test coupling of ethyl 4-bromobenzoate with N-methylpyrrole (in the presence of DIPEA and **PTh-OMe**), which we used as the case study.

Figure S8 shows the as prepared emulsions with the five surfactants.

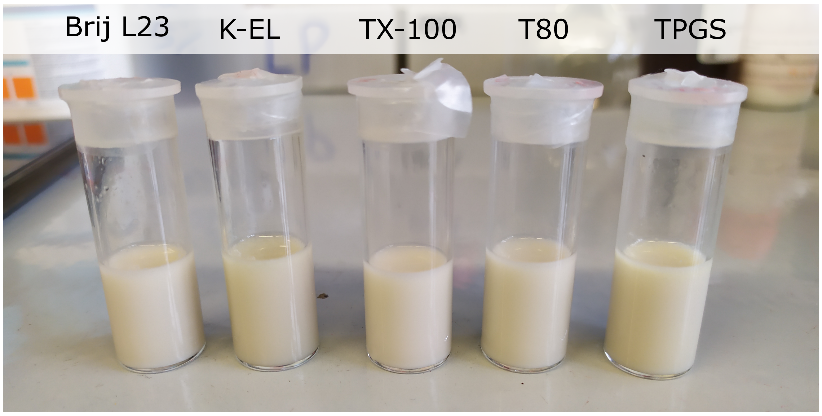

Figure S8 As prepared emulsions of ethyl 4-bromobenzoate, N-methylpyrrole, DIPEA and **PTh-OMe** in 2 wt% aqueous solutions of different surfactants (from left to right: Brij L23, Kolliphor EL, Triton X-100, Tween 80, TPGS-750-M).

---

*This requirement is way less stringent for the Corning® Lab Photo Reactor, as it ensures continuous mixing. See also Section 9.

The as prepared five emulsions look identical. If allowed to stand without being mixed or stirred, phase separation starts to occur. Figure S9 shows the same emulsions 48 hours after emulsification. Emulsion prepared with BL23 shows a clear phase separation, which starts only a few minutes after emulsification. The emulsion prepared using TPGS separates as well, although in little extent. The emulsion prepared with TX100, the most homogeneous at time zero, starts separating after 24 hours, ending in a clear flocculation of the organic phase. Both the emulsions prepared with K-EL and T80 lasted for a longer time, the latter showing signs of flocculation only after 48 hours.

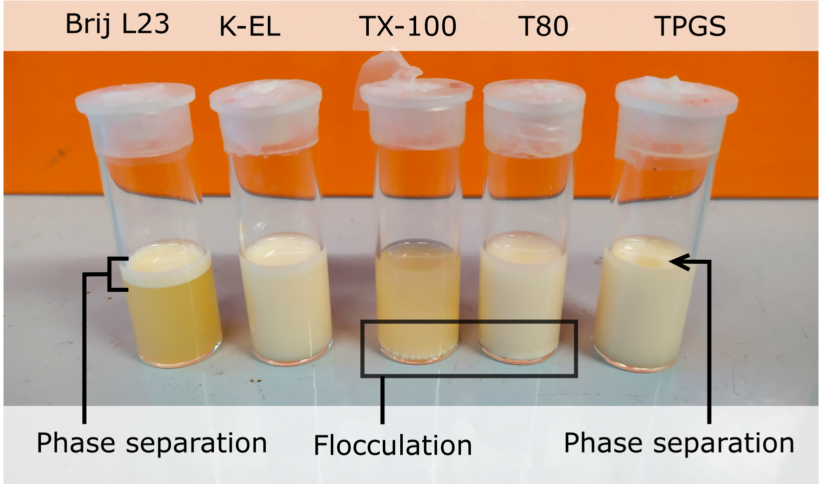

Figure S9 Picture of the emulsions of ethyl 4-bromobenzoate, N-methylpyrrole, DIPEA and **PTh-OMe** in 2 wt% aqueous solutions of different surfactants (from left to right: Brij L23, Kolliphor EL, Triton X-100, Tween 80, TPGS-750-M) 48 hours after emulsification.

7 Calculation of GC-MS relative response factors

We quantified the composition of reactions reported in Table 1 and Table 2 in terms of aryl bromide R, hydrodehalogenation product H, cross-coupling product P and double coupling product DP by gas chromatography coupled with mass spectroscopy (GC-MS). We estimated the reaction mixture composition through area normalization based on relative response factors method.

In order to obtain the relative response factors f_x of the different compounds, we prepared four standard solutions at known molar concentration of the pure compounds in dichloromethane in a volumetric flask. Each standard solution was analyzed three times by GC-MS.

Areas of each peak A_x were normalized by the weight of the corresponding compound W_x, and relative response factors were obtained using the following formula (s labels the standard)

$$f_x = f_s \cdot \frac{A_s}{A_x} \cdot \frac{W_x}{W_s}$$

We decided to use the product as standard, thus

$$f_s = f_P = 1$$

and using the previous equation, we found the relative response factor of the reagent f_R, the hydrodehalogenation product f_H, and double coupling product f_{DP}, which are reported in the following table.

f_R	f_H	f_{DP}
1.16 ± 0.02	1.26 ± 0.01	0.94 ± 0.02

Weight percentage ($W\%$) and mole percentage ($n\%$) of each component were therefore calculated as

$$W\%_x = \frac{f_x A_x^{sample}}{\sum f_x A_x^{sample}} \cdot 100$$

$$n\%_x = \frac{{W\%_x}/{MW_x}}{\sum {W\%_x}/{MW_x}} \cdot 100$$

where A_x^{sample} is compound x peak area in sample solution and MW_x is its molecular weight.

8 Impact of scattering on the optimization of reactions performed with the Corning® Lab Photo Reactor

All the reactions performed using water as the medium have emulsions features. The volume of organics in fact is around 1/10 of the volume of water, way above the amount that can be micellized by the surfactant. Figure S10A shows the typical aspect of an as-prepared reaction mixture before illumination: the mixture is opaque due to the light scattered by the organics droplets suspended within the aqueous phase. Figure S10B shows the transmission spectrum of this emulsion collected in a 1 mm thick cuvette (inset of Figure S10B), compared with the spectrum of an identical reaction mixture prepared in acetonitrile instead of water.

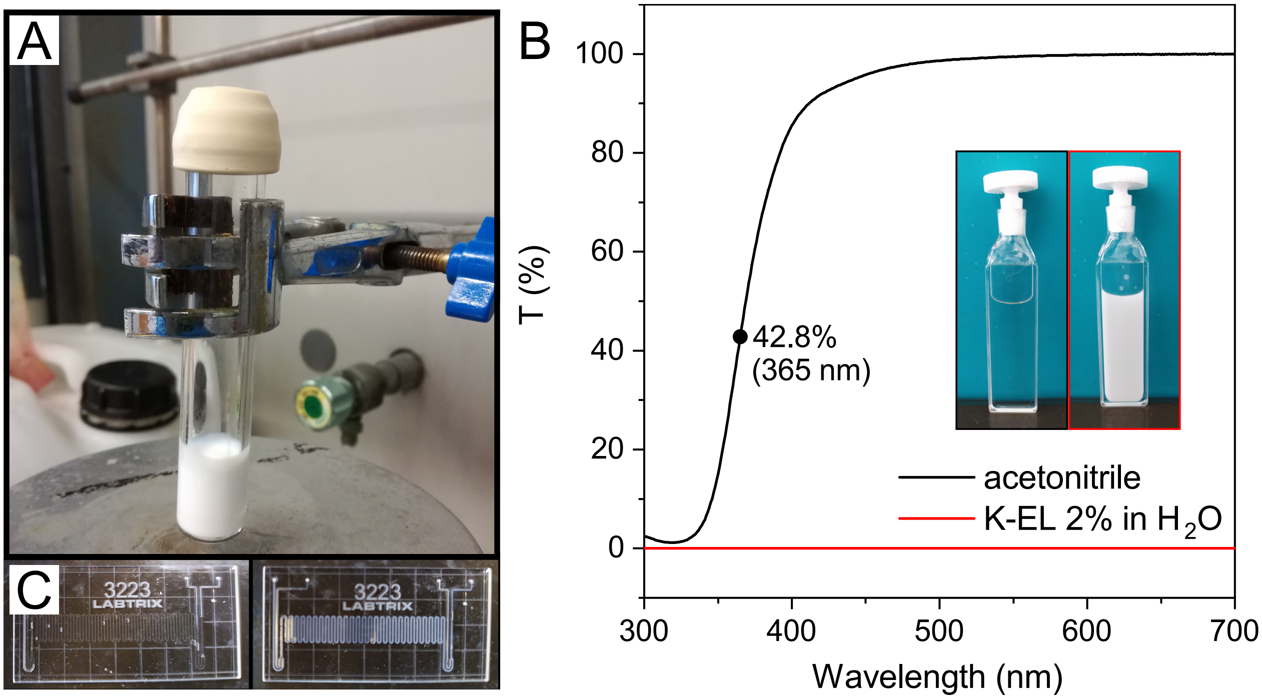

Figure S10 A) Aspect of the emulsion obtained after sonication of ethyl 4-bromobenzate, N-methylpyrrole, DIPEA and **PTh-OMe** in 2 wt% K-EL aqueous medium. B) Transmission spectrum of the mixture shown in Figure S10a, compared with the transmission spectrum of an identical reaction mixture prepared in acetonitrile. Both spectra were collected in a 1 mm glass cuvette. The inset shows the pictures of the cuvette containing the corresponding reaction mixture. C) Picture of a micro reactor (Labtrix 3223, channel thickness: 120 µm) containing the reaction mixture prepared in acetonitrile (left) or aqueous 2 wt% K-EL (right).

In acetonitrile, the transmittance is less than 90% only below 400 nm, due to the absorption of **PTh-OMe** photocatalyst (transmission minimum is observed at 320 nm, corresponding to photocatalyst absorption maximum, see Figure S4). The heterogeneous aqueous 2 wt% K-EL mixture has instead zero transmittance over the whole measured spectrum. Light is not absorbed by the medium (as no species are present which can absorb light above 400 nm), but it is lost due to scattering.

The channels of the Corning® Lab Photo Reactor are thinner than 1 mm, therefore scattering is reduced, but not eliminated. In fact, scattering is observable even in channels thinner than those of the Corning® Lab Photo Reactor (as demonstrated by Figure S10C, showing the emulsion in the Labtrix 3223 microreactor, featuring channel thickness of 120 µm). Such opacity makes light losses unavoidable, and extremely difficult to be estimated. Therefore, optimization of catalyst concentration using the Lambert-Beer law[S7] was not possible, because the Lambert-Beer law can be applied only to fully transmitting media. A modified Lambert-Beer law accounting for scattering effects exist, which is for example applied in cellular imaging due to scattering arising from tissues.[S8] However, its application requires the precise knowledge of the increment of effective pathlength of light due to scattering, and of the geometry of the measurement equipment. The application of such modified Lambert-Beer law to our system is unpractical, and it falls out of the scope of the present work.

We instead checked if we could run the reactions at lower power density. Figure S11 shows the advancement of the coupling reaction between ethyl 4-bromobenzate and N-methylpyrrole performed at 50% and 70% LEDs light intensity (radiant flux of 21.8 W and 30.5 W respectively).

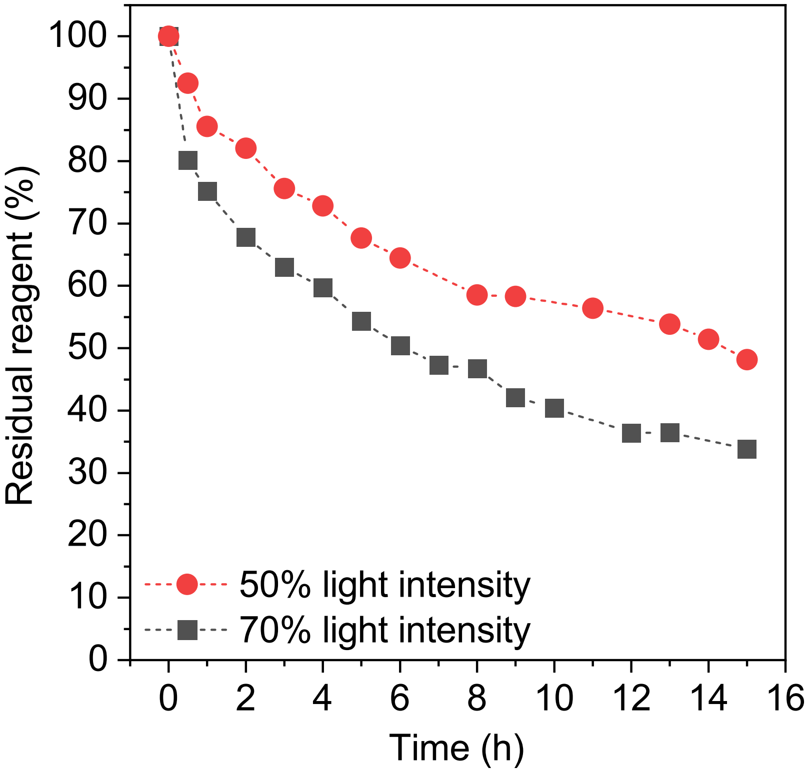

Figure S11 Conversion curves for the reaction of ethyl 4-bromobenzoate with N-methylpyrrole performed at 50% and 70% LEDs light intensity in the Corning® Lab Photo Reactor. Error bars (±2%) are omitted, as they fall within the respective symbols.

Reaction performed at 50% light intensity is slower than that performed at 70% light intensity. We did not check if raising the radiant flux would lead to a further increase of the reaction speed, as this is the maximum recommended value from the LEDs supplier for long running experiments.

9 Reproducibility of reactions in emulsion run in the Corning® Lab Photo Reactor

Reactions run in emulsion conditions might suffer of reproducibility issues[S6] due to well known tendency of emulsions to flocculation and creaming.[S9] To test reproducibility obtained with the Corning® Lab Photo Reactor, we repeated the reaction between ethyl 4-bromobenzoate and N-methylpyrrole four times under the same conditions. Residual halide amount was monitored for 15 hours at most through GC-MS analysis every 1 or 2 hours for each test. Curves of the residual halide amount over time are reported in figure S12, and they result essentially identical, highlighting the optimal reproducibility obtained with such photochemical setup.

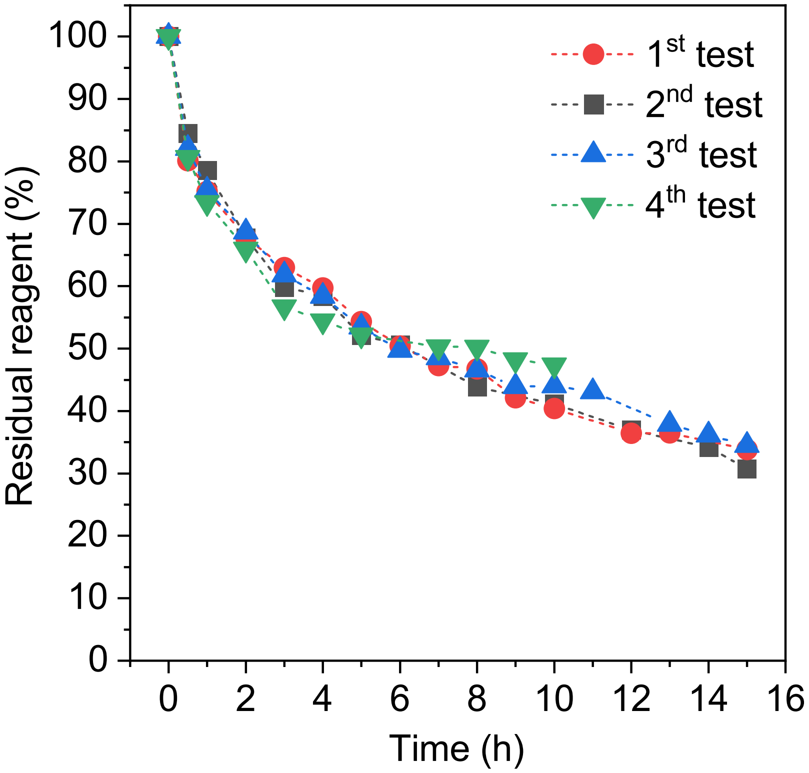

Figure S12 Conversion curves of ethyl 4-bromobenzoate for four reactions performed in the Corning® Lab Photo Reactor under the same working conditions. Error bars (±2%) are omitted for clarity.

10 Dependence of reaction rate from hydrophilicity of the base

In presence of a lipophilic tertiary amine (such as DIPEA), a hydrophilic tertiary amine (such as TEA) or an inorganic base, the ethyl 4-bromobenzoate conversion proceeds at different rates, as shown in Figure S13. In particular, the reaction slows down with increasing base hydrophilicity. At the same time, an increase of the selectivity of the reaction toward the coupling product is also observed (see data in Table 2).

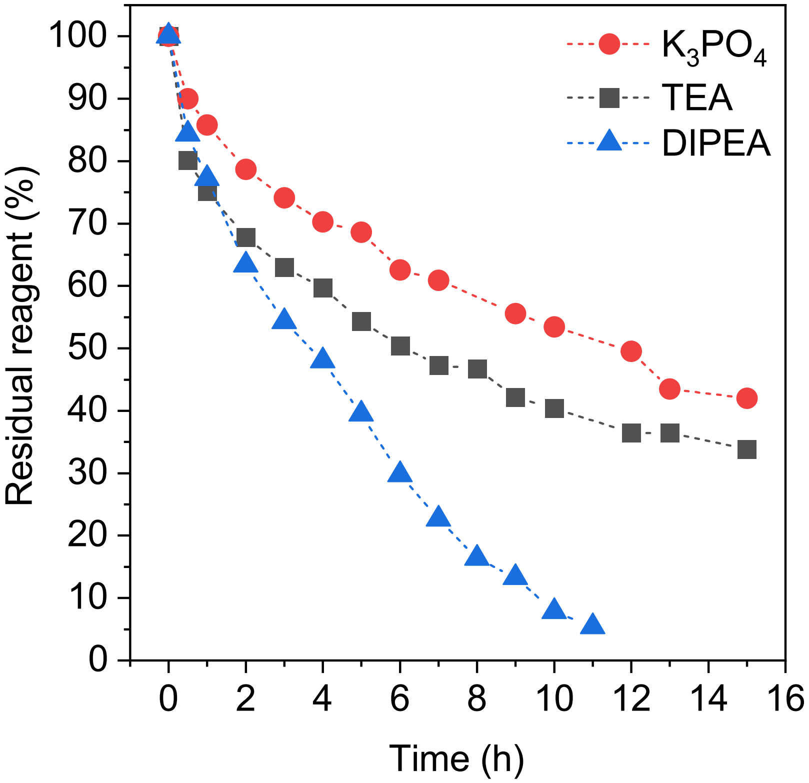

Figure S13 Progress of ethyl 4-bromobenzoate conversion when DIPEA, TEA or K_3PO_4 are used as the bases in the test reaction. Error bars (±2%) are omitted, as they fall within the respective symbols.

A tentative explanation of these observation is given, based on the accessible and hindered pathways of the catalytic cycle shown in cartoons in Figure 2 in the main text.

11 GC-MS traces for reactions reported in Scheme 2 and Scheme 4

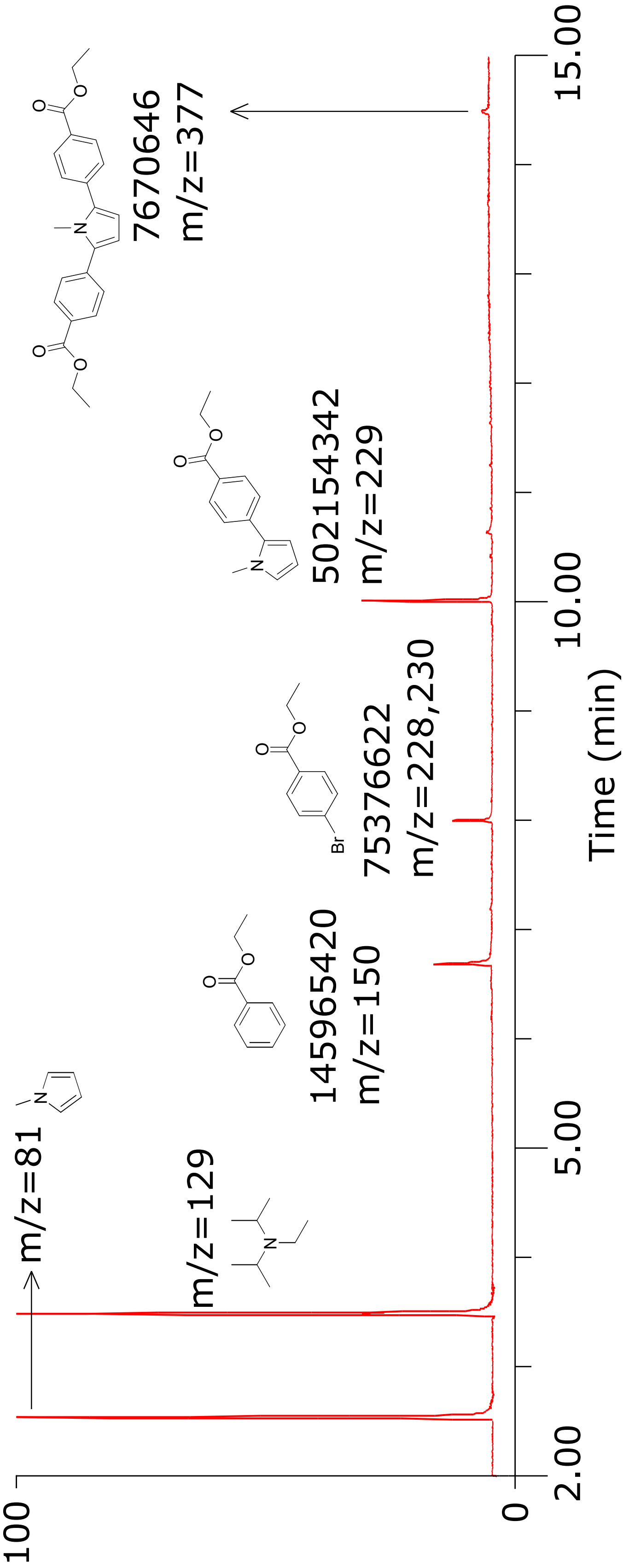

Figure S14 GC-MS chromatogram for the reaction in Scheme 2 to obtain product **1**

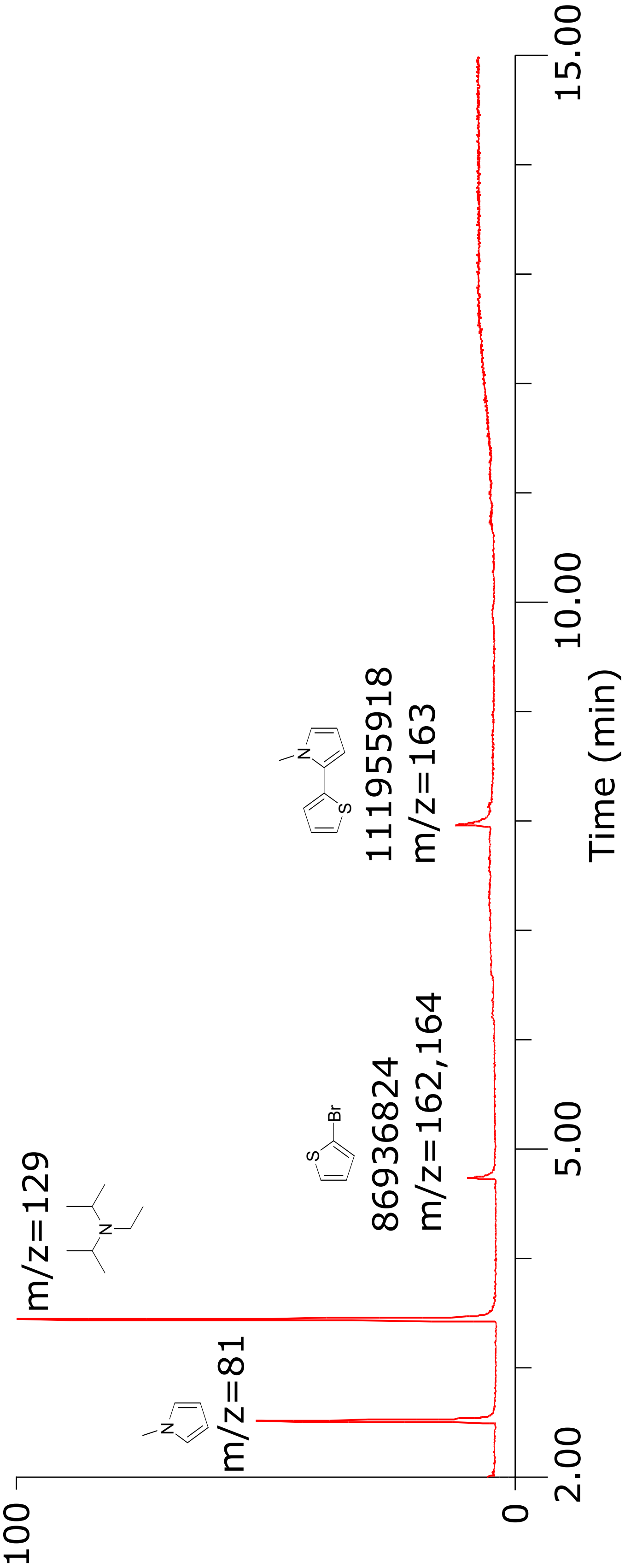

Figure S15 GC-MS chromatogram for the reaction in Scheme 2 to obtain product **4**

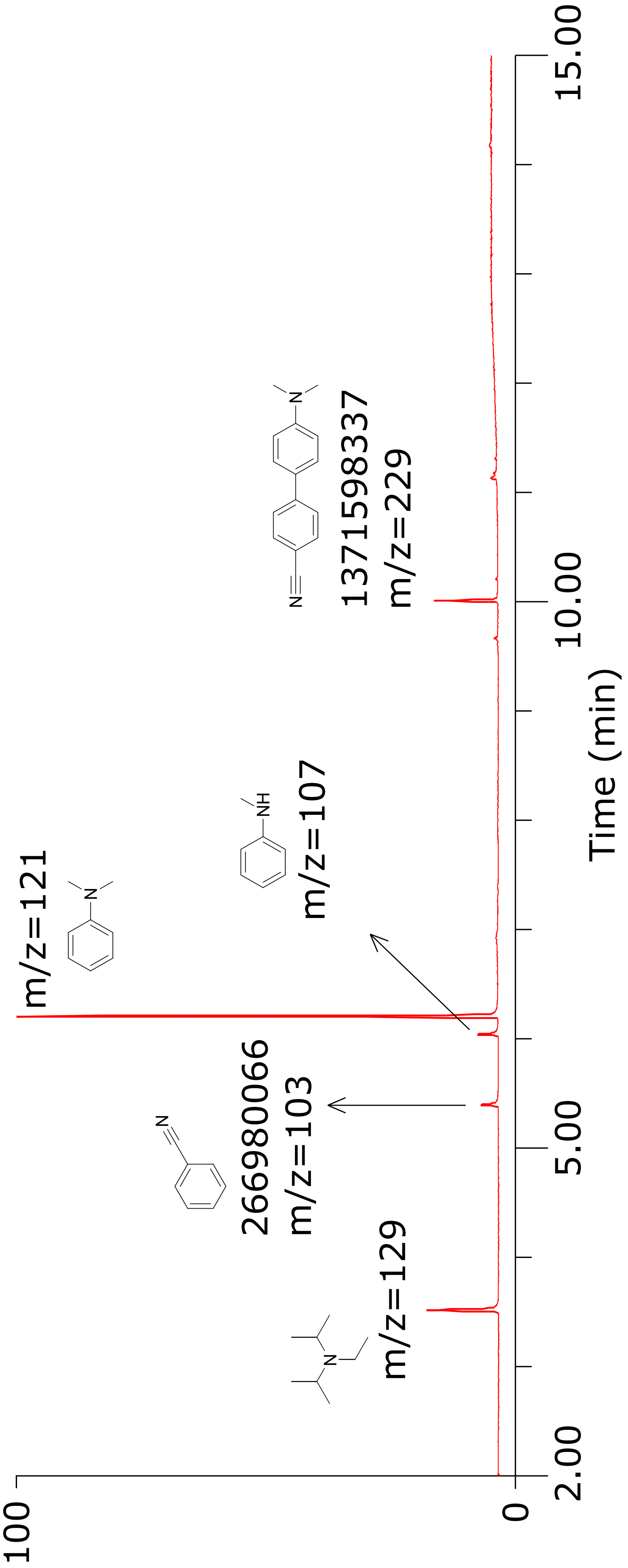

Figure S16 GC-MS chromatogram for the reaction in Scheme 2 to obtain product **5**

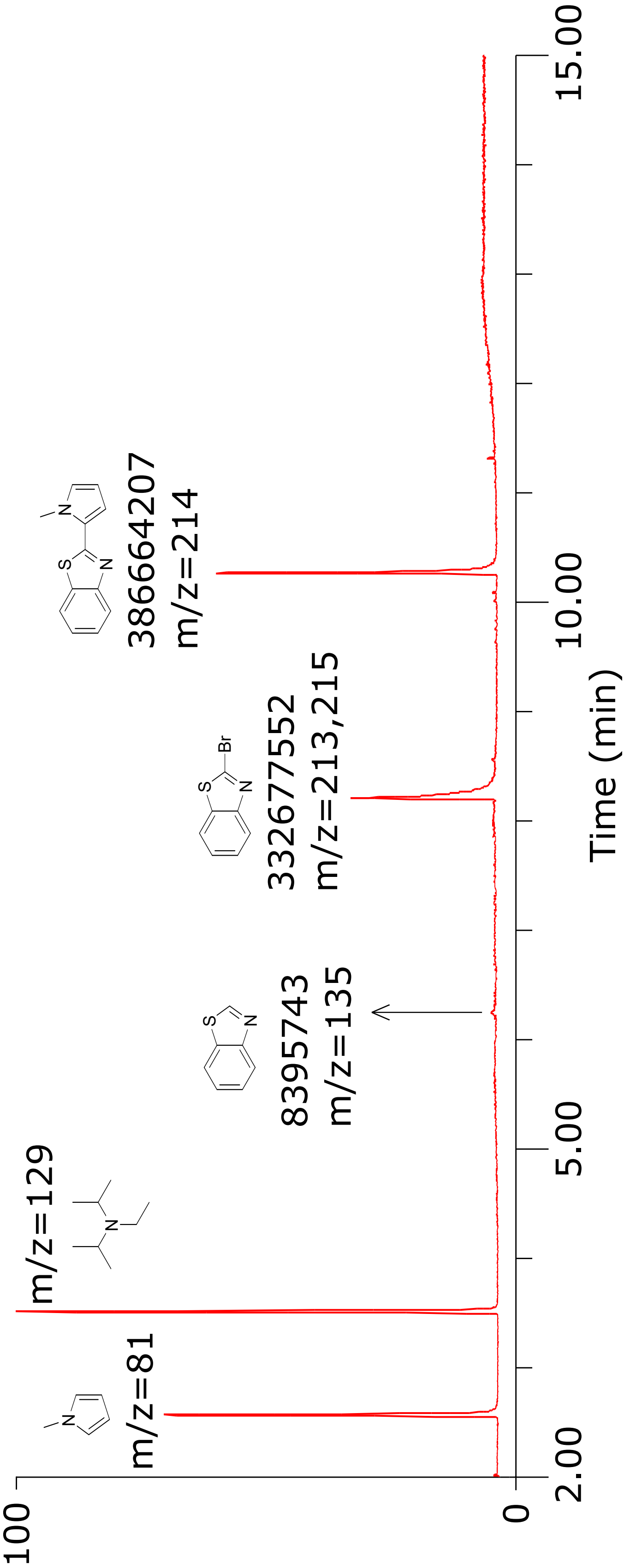

Figure S17 GC-MS chromatogram for the reaction in Scheme 2 to obtain product **6**

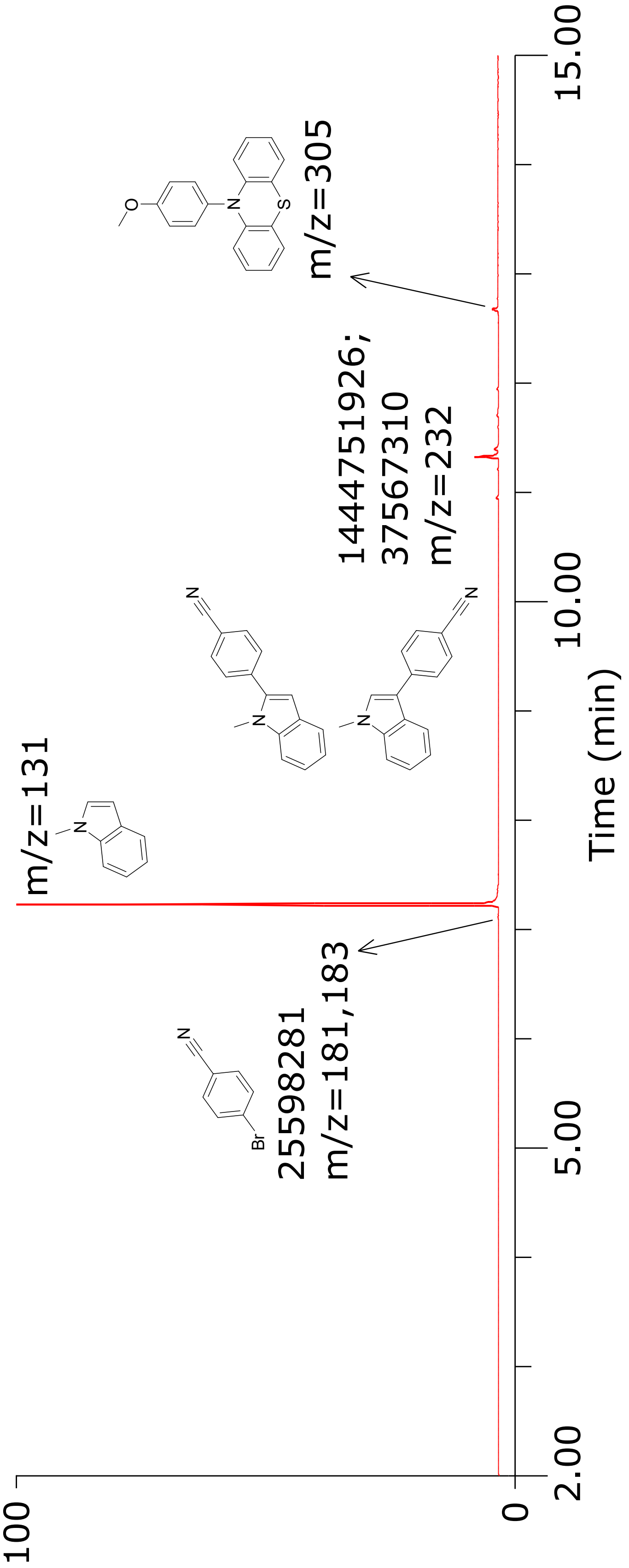

Figure S18 GC-MS chromatogram for the reaction in Scheme 2 to obtain product **7** (setup b)

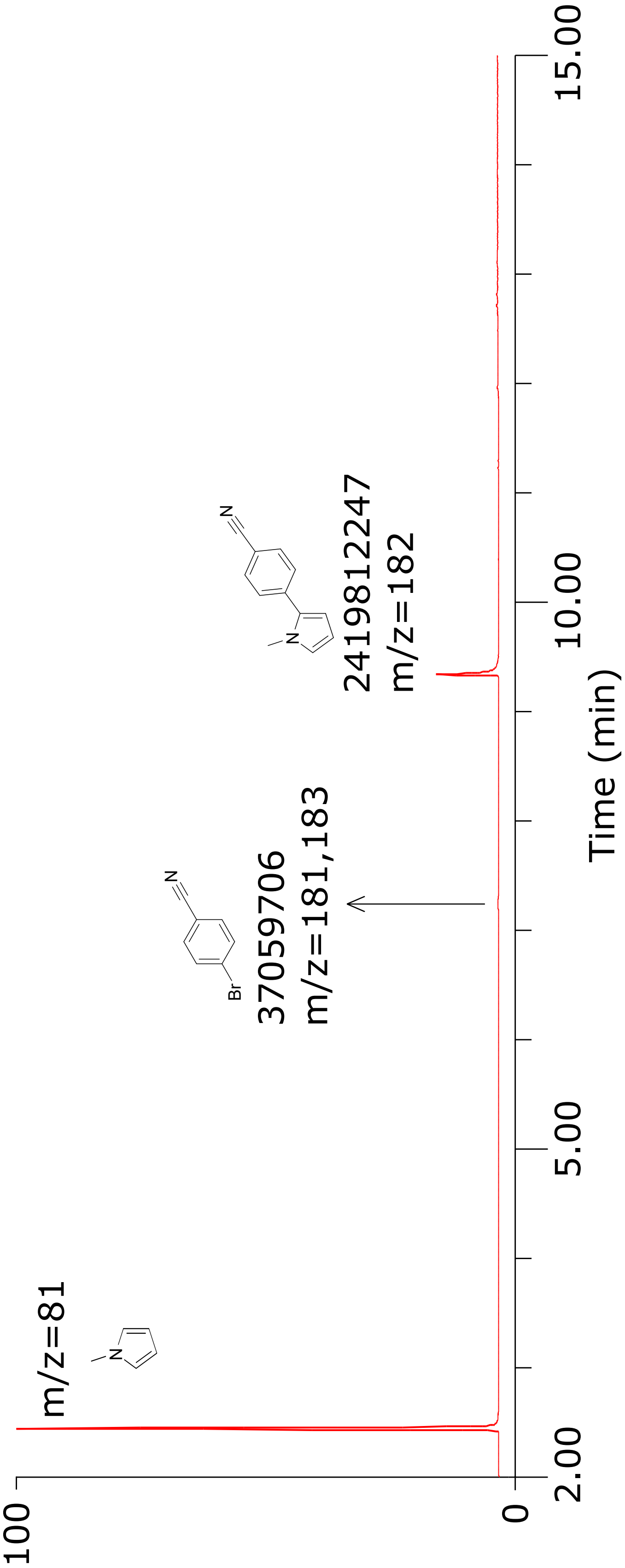

Figure S19 GC-MS chromatogram for the reaction in Scheme 2 to obtain product **8** (setup b)

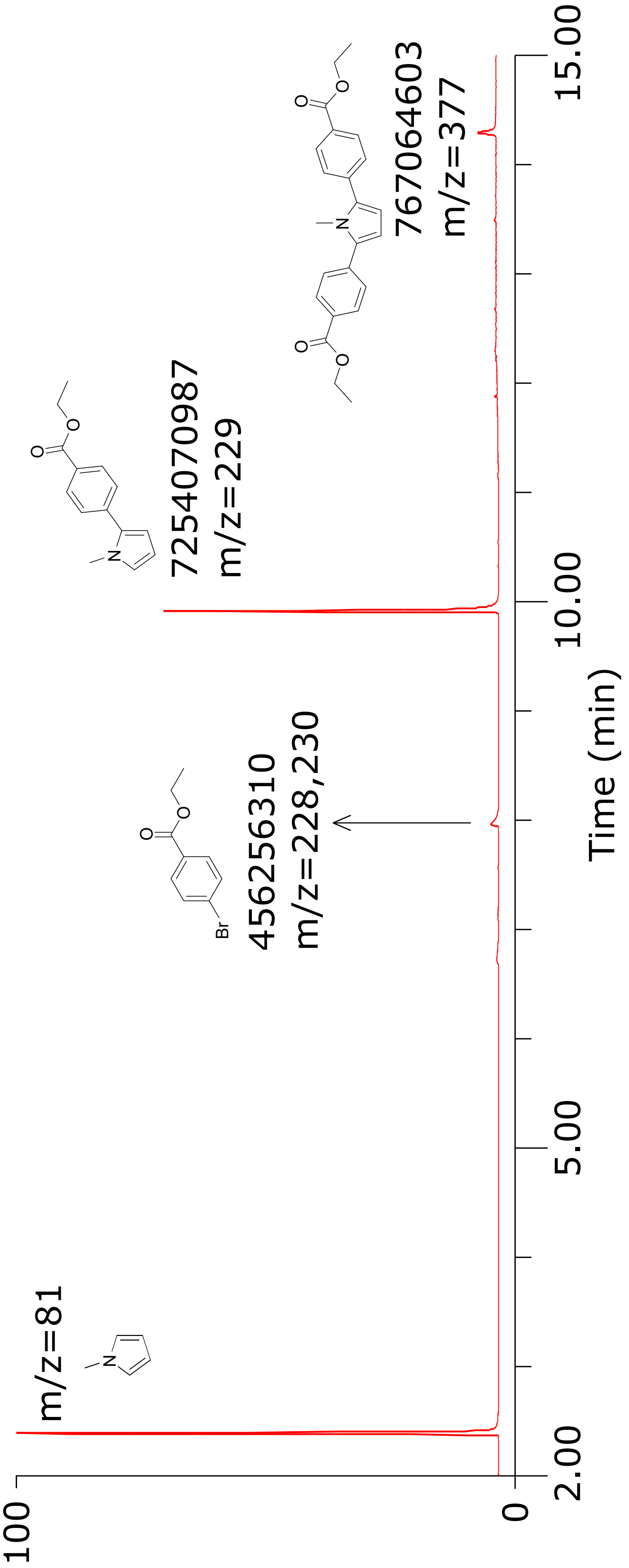

Figure S20 GC-MS chromatogram for the reaction in Scheme 4 to obtain product **1** (setup a)

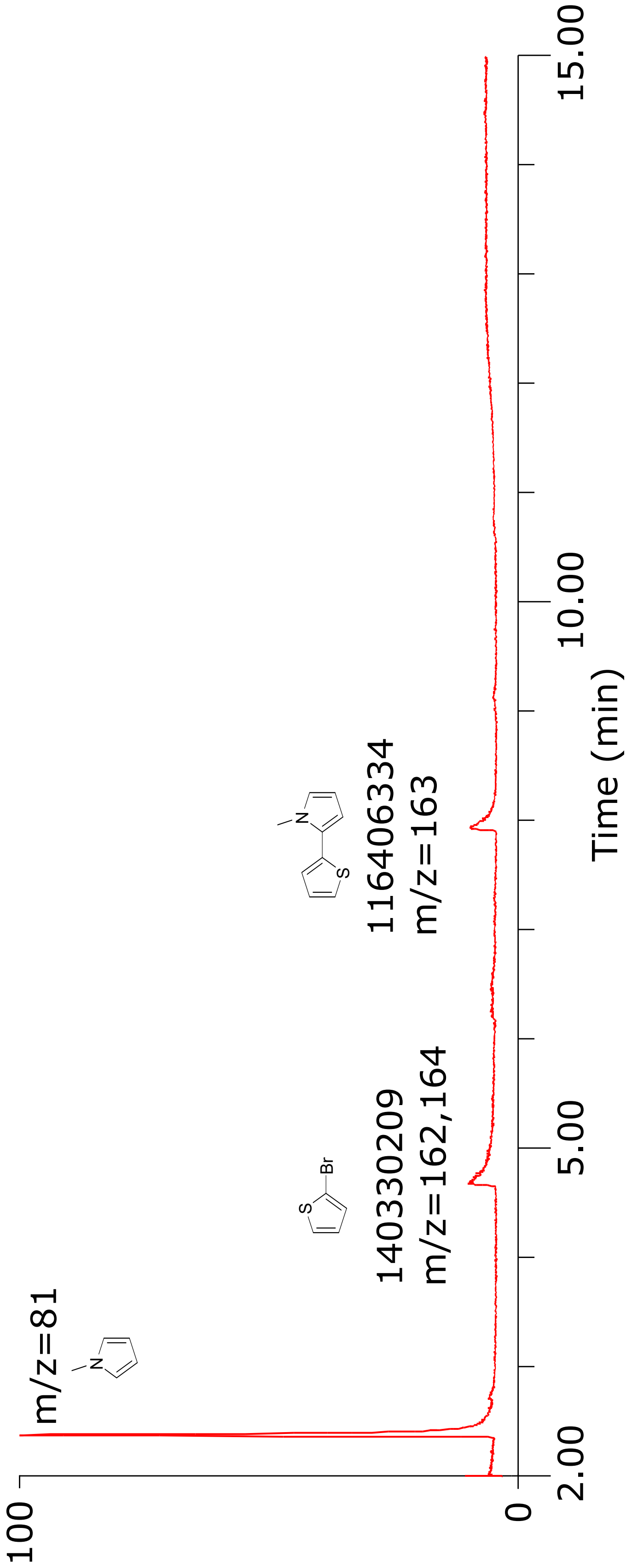

Figure S21 GC-MS chromatogram for the reaction in Scheme 4 to obtain product **4**

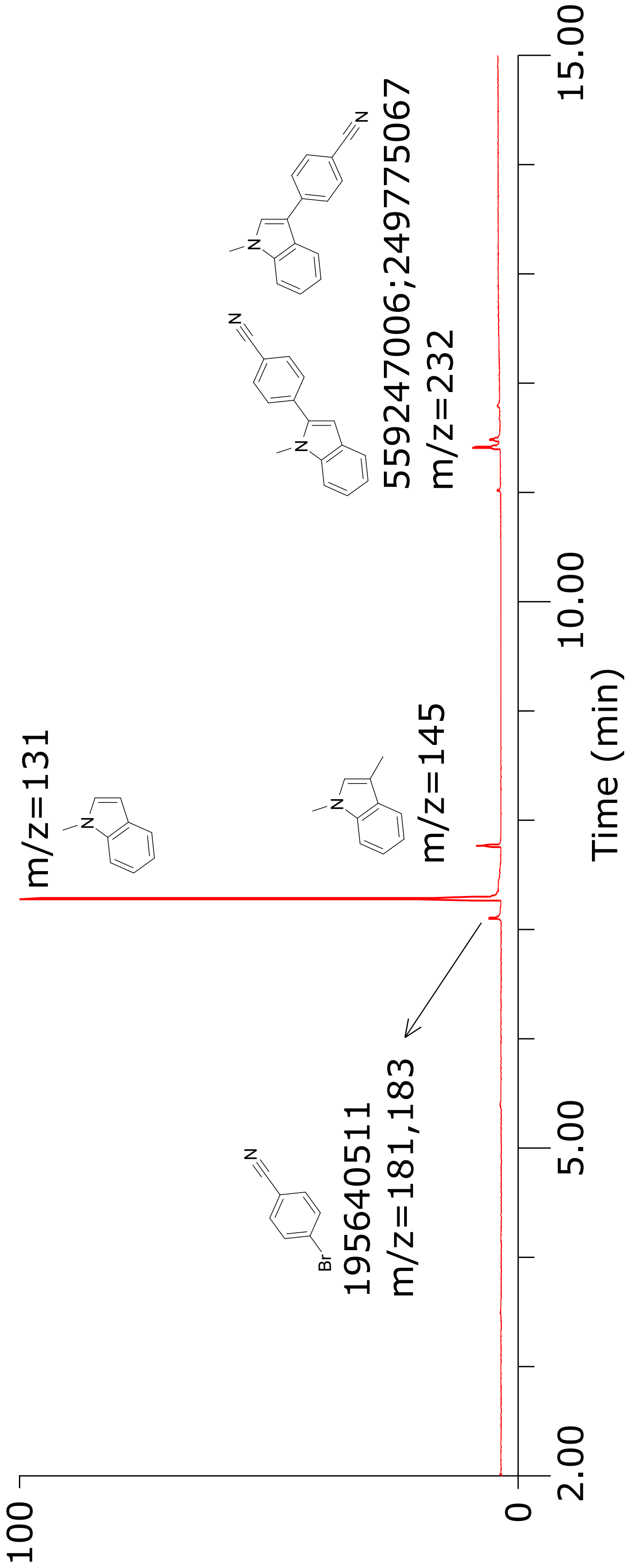

Figure S22 GC-MS chromatogram for the reaction in Scheme 4 to obtain product **7**

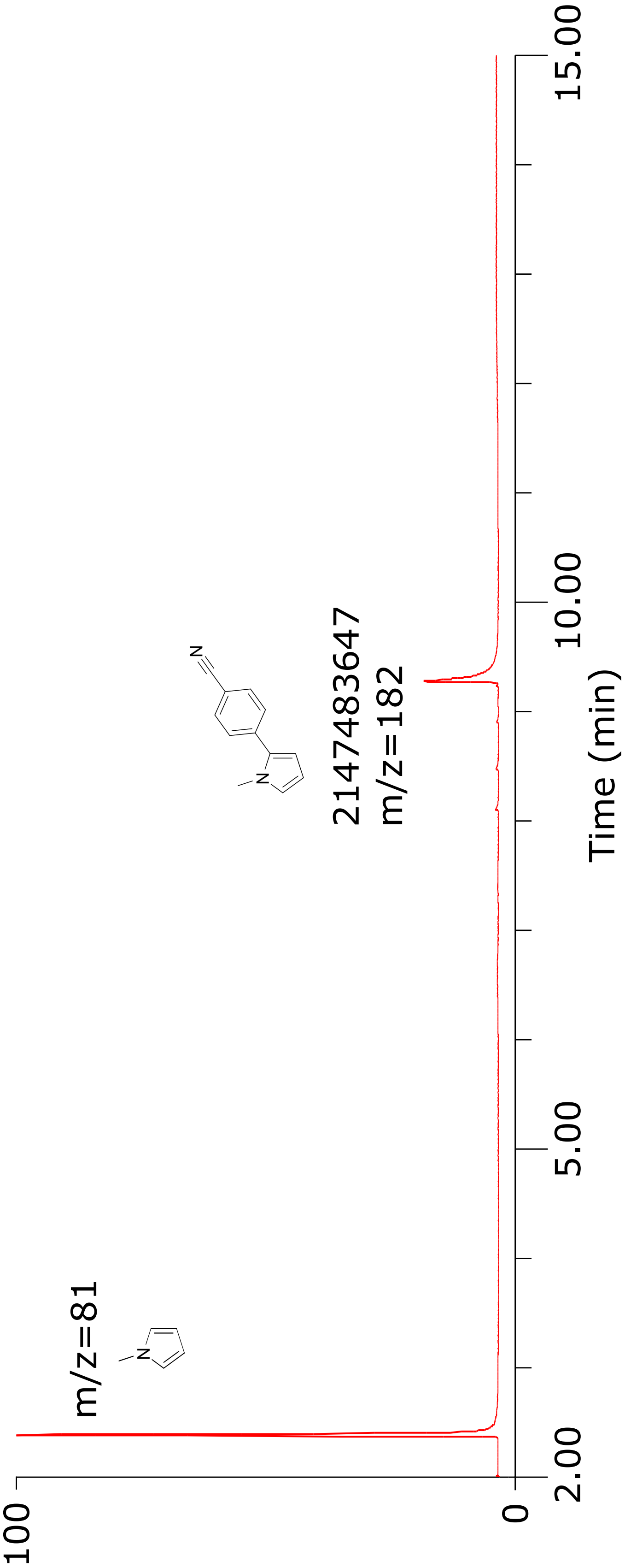

Figure S23 GC-MS chromatogram for the reaction in Scheme 4 to obtain product **8**

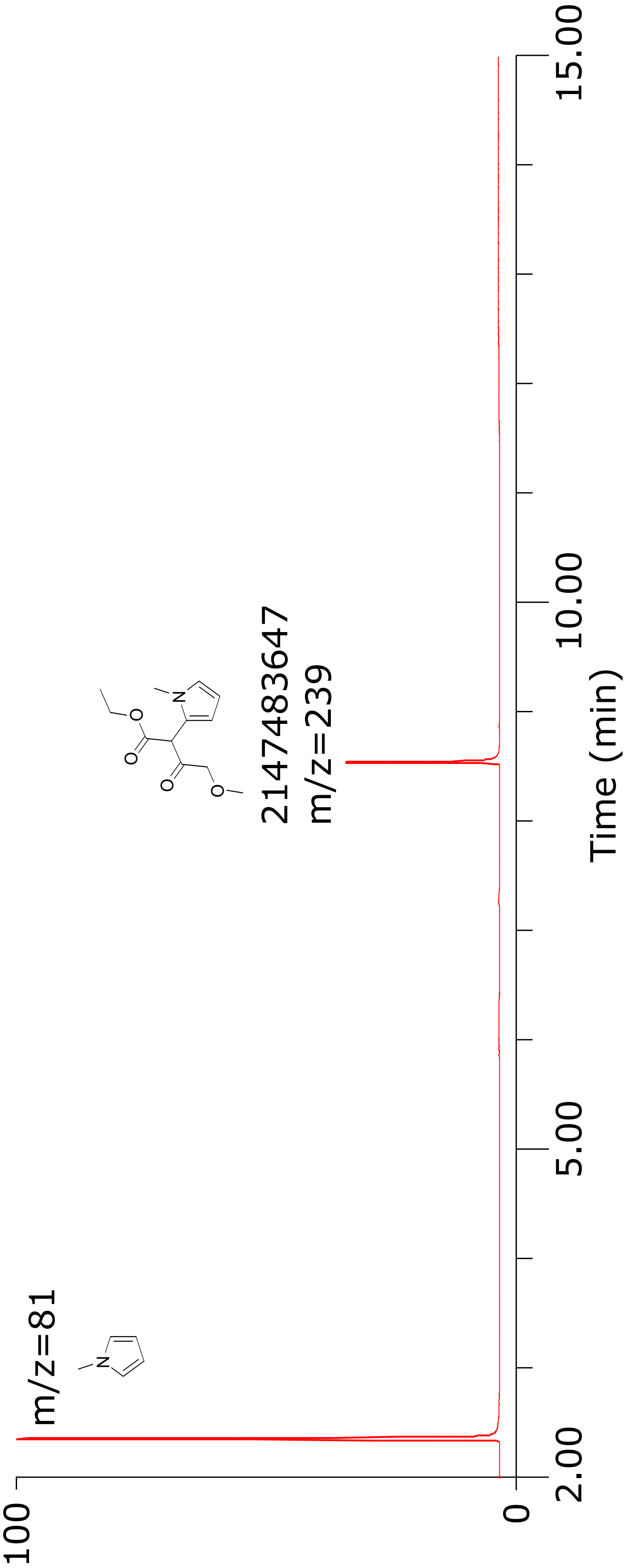

Figure S24 GC-MS chromatogram for the reaction in Scheme 4 to obtain product **9**

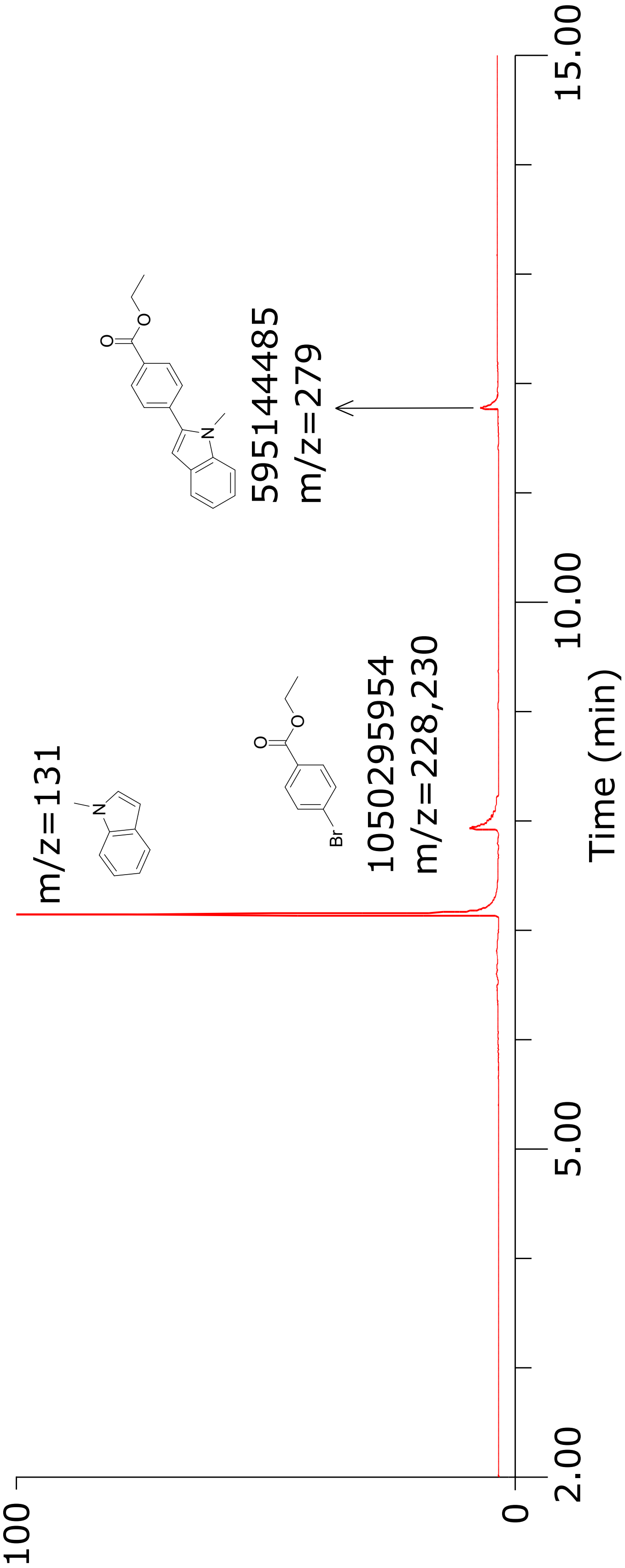

Figure S25 GC-MS chromatogram for the reaction in Scheme 4 to obtain product **10**

12 NMR spectra of new and known derivatives

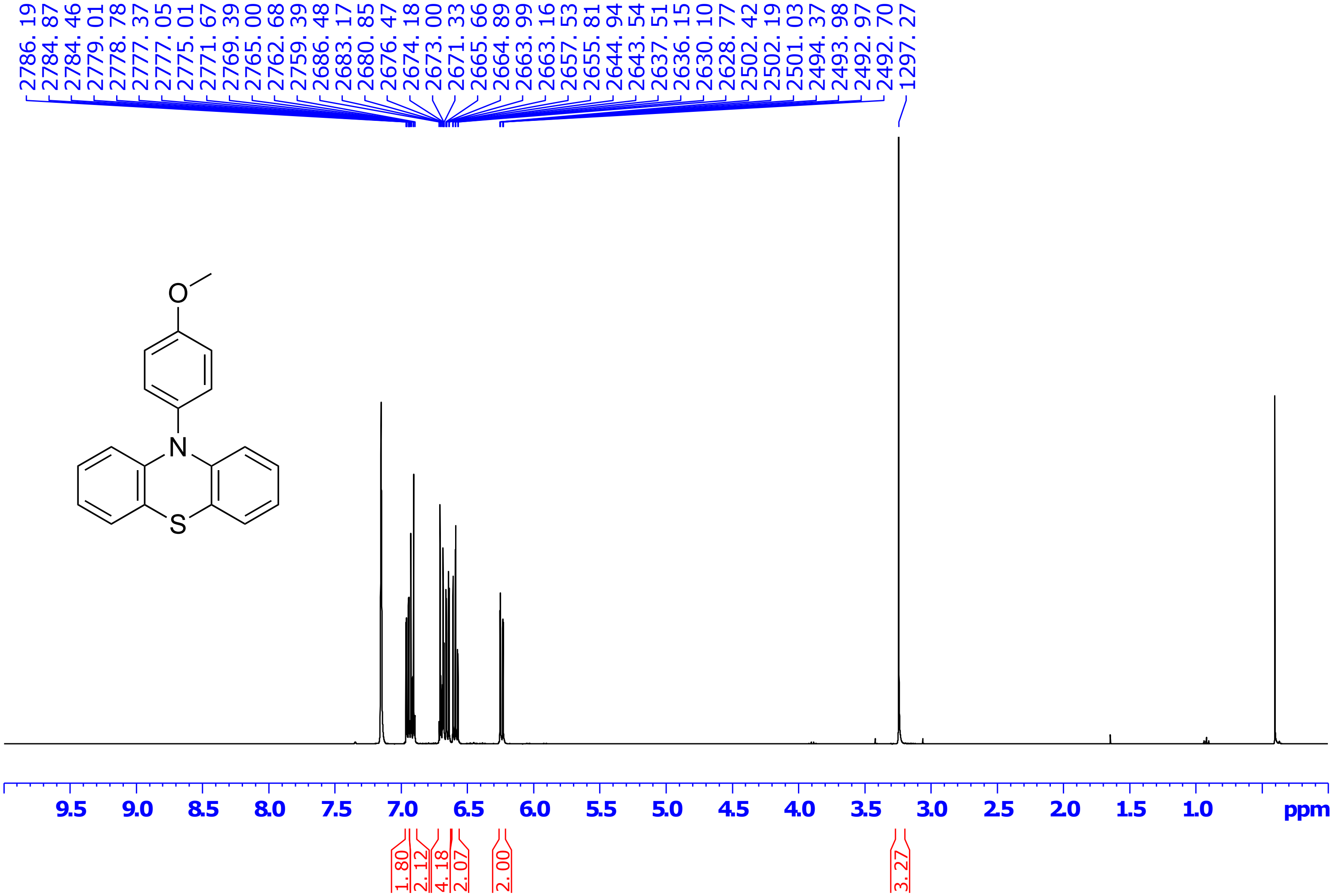

Figure S26 ^{1}H NMR of derivative **PTh-OMe** in benzene-d$_6$.

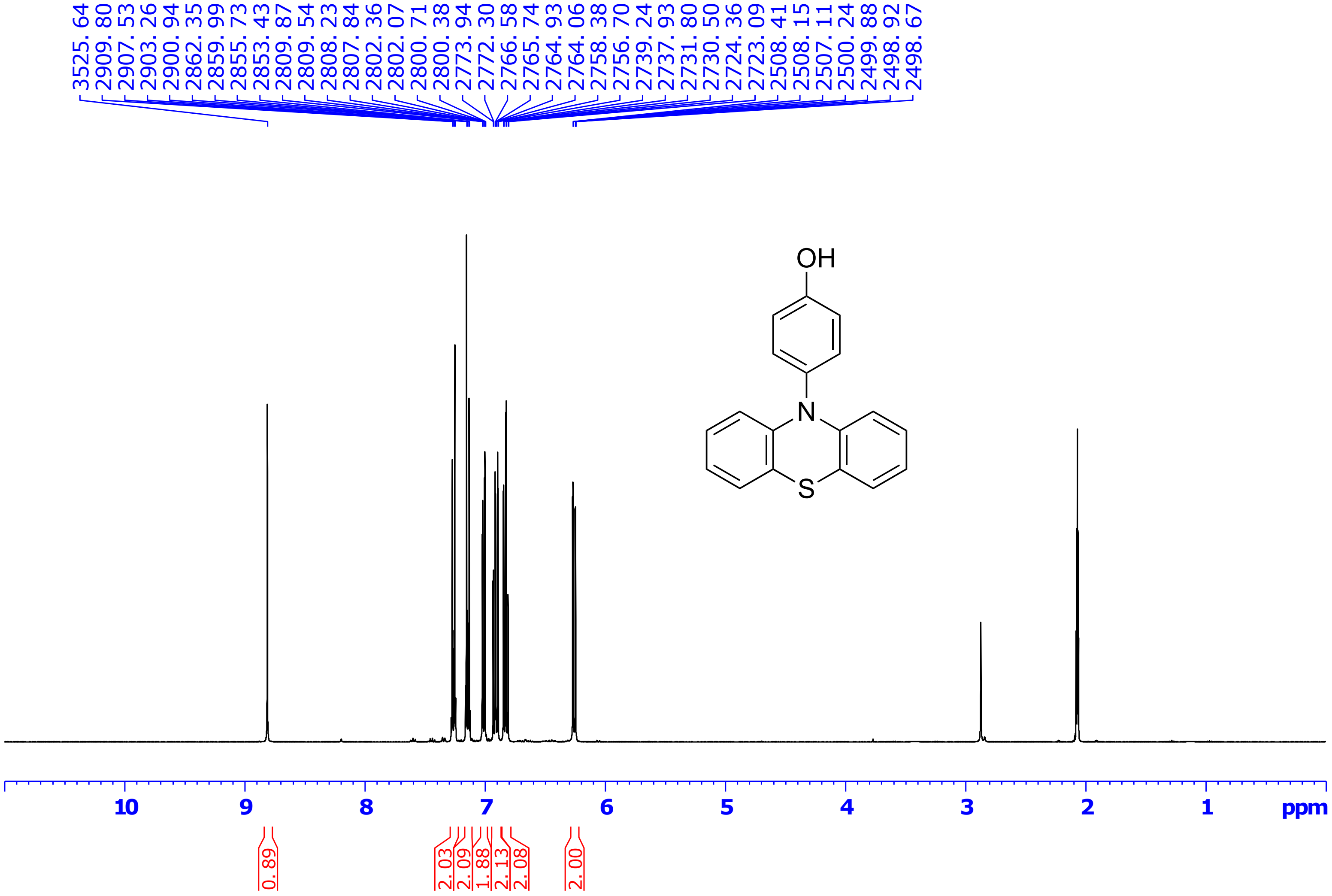

Figure S27 ^{1}H NMR of derivative **11** in acetone-d$_6$.

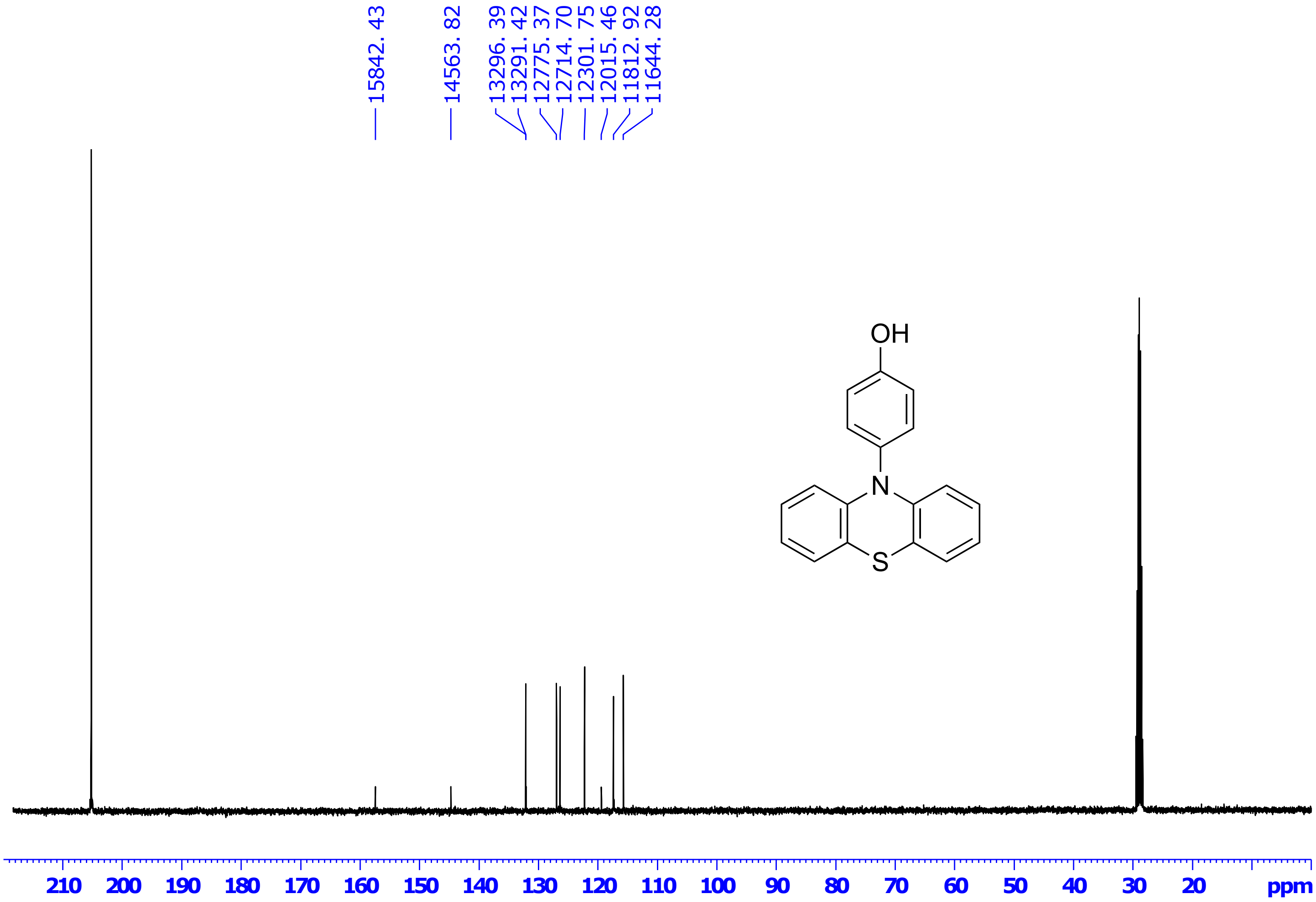

Figure S28 ^{13}C NMR of derivative **11** in acetone-d$_6$.

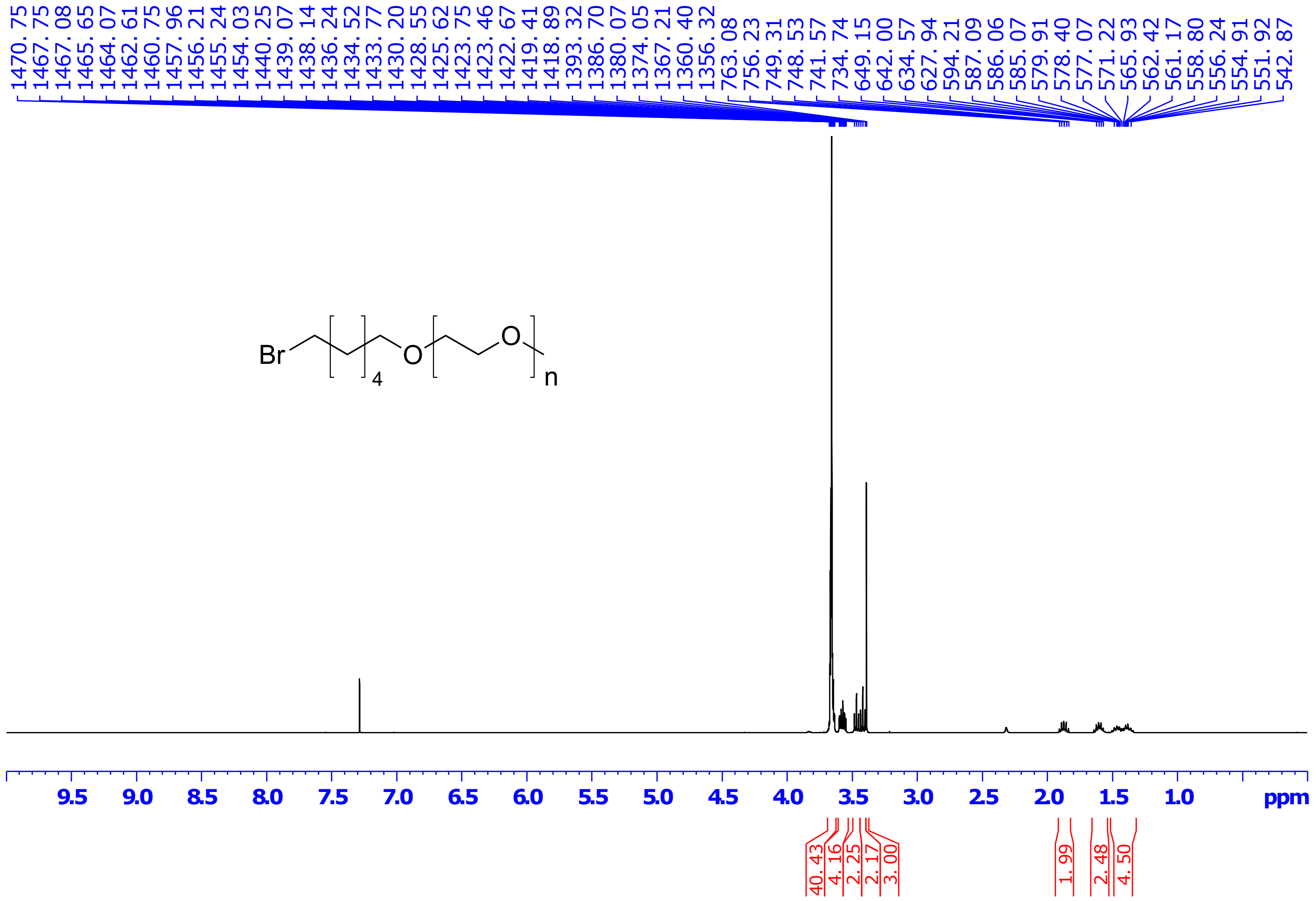

Figure S29 ^{1}H NMR of derivative **12** in CDCl$_3$.

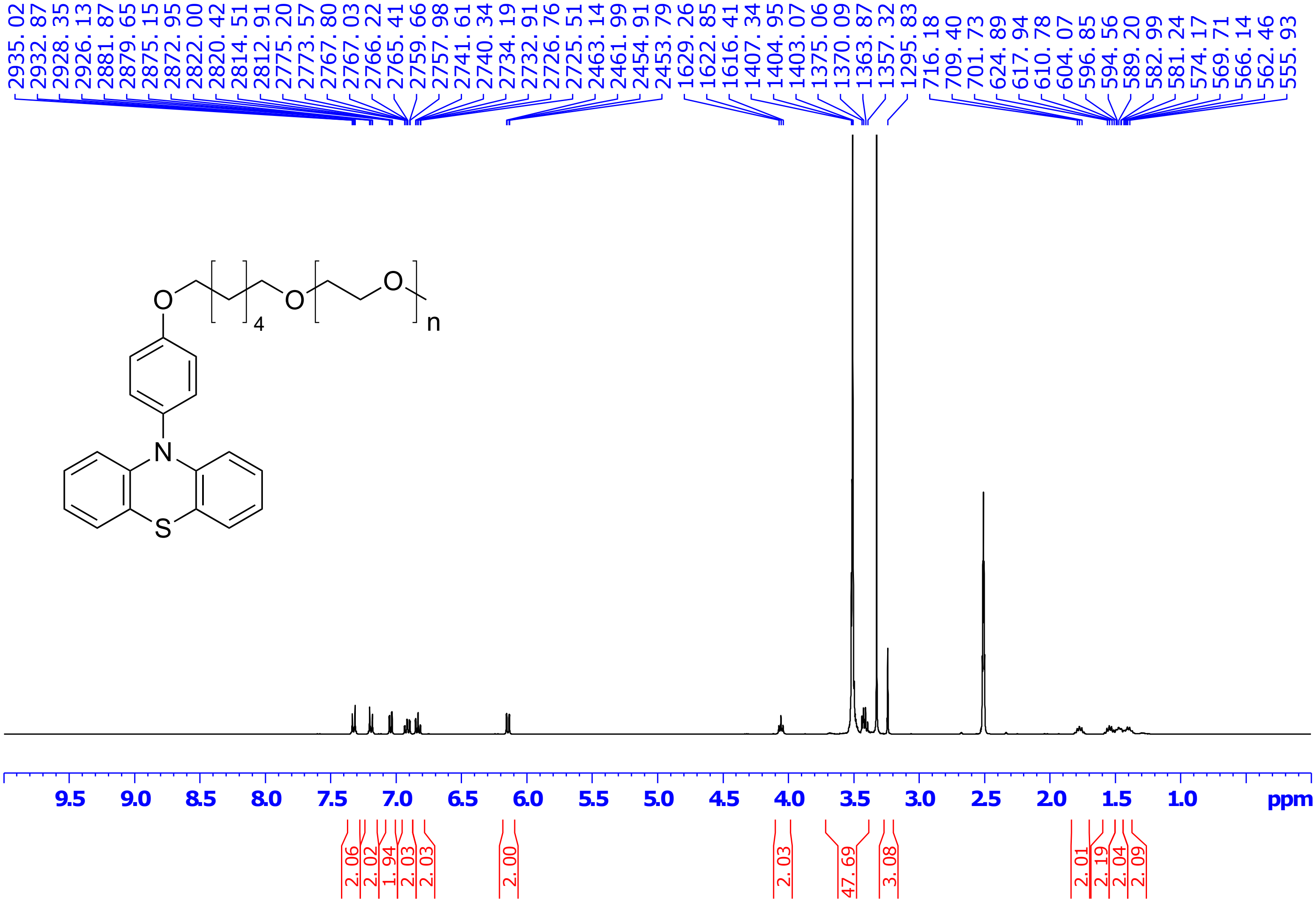

Figure S30 ^{1}H NMR of derivative **S-PTh** in DMSO-d$_6$.

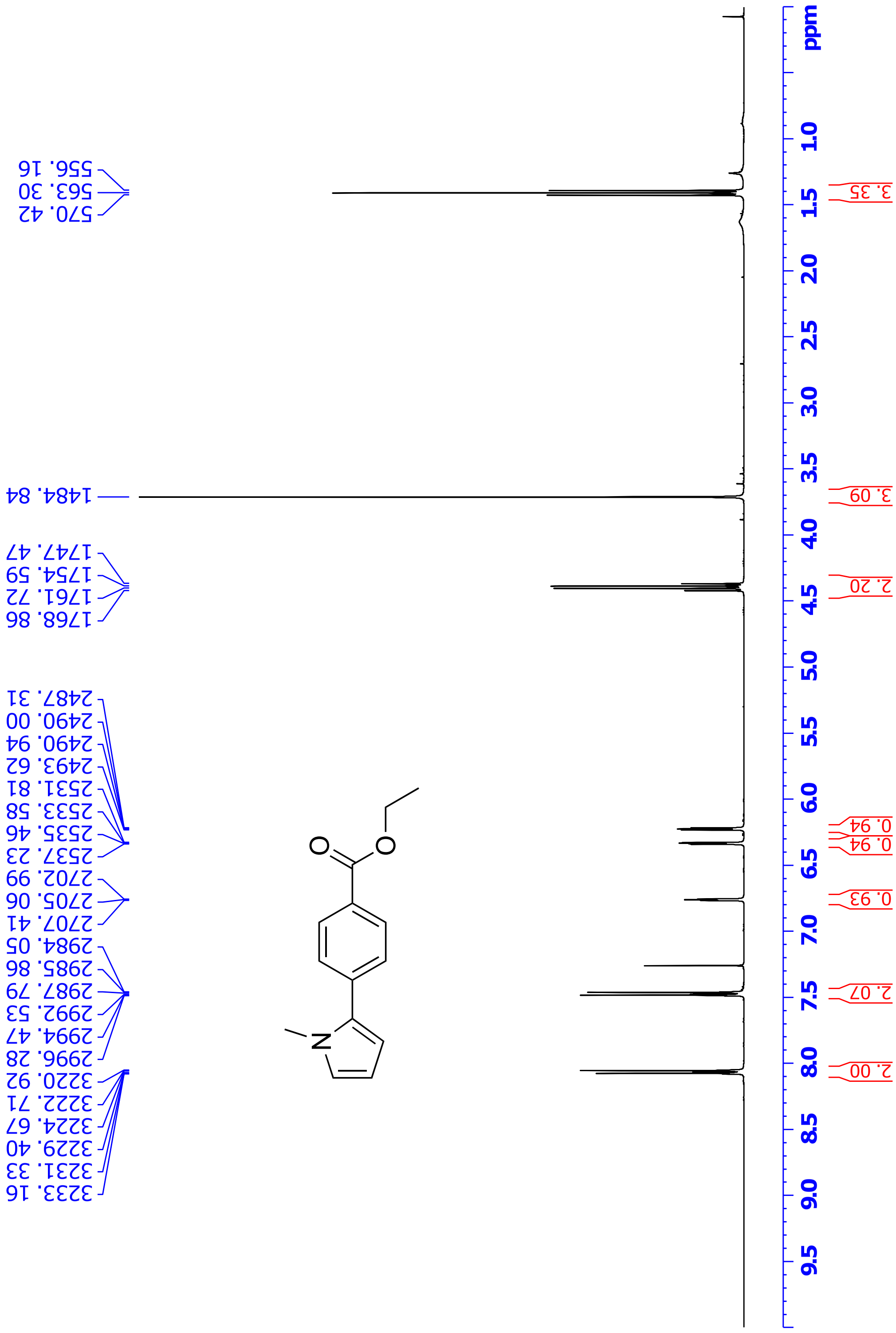

Figure S31 ^{1}H NMR of derivative **1** in $CDCl_3$.

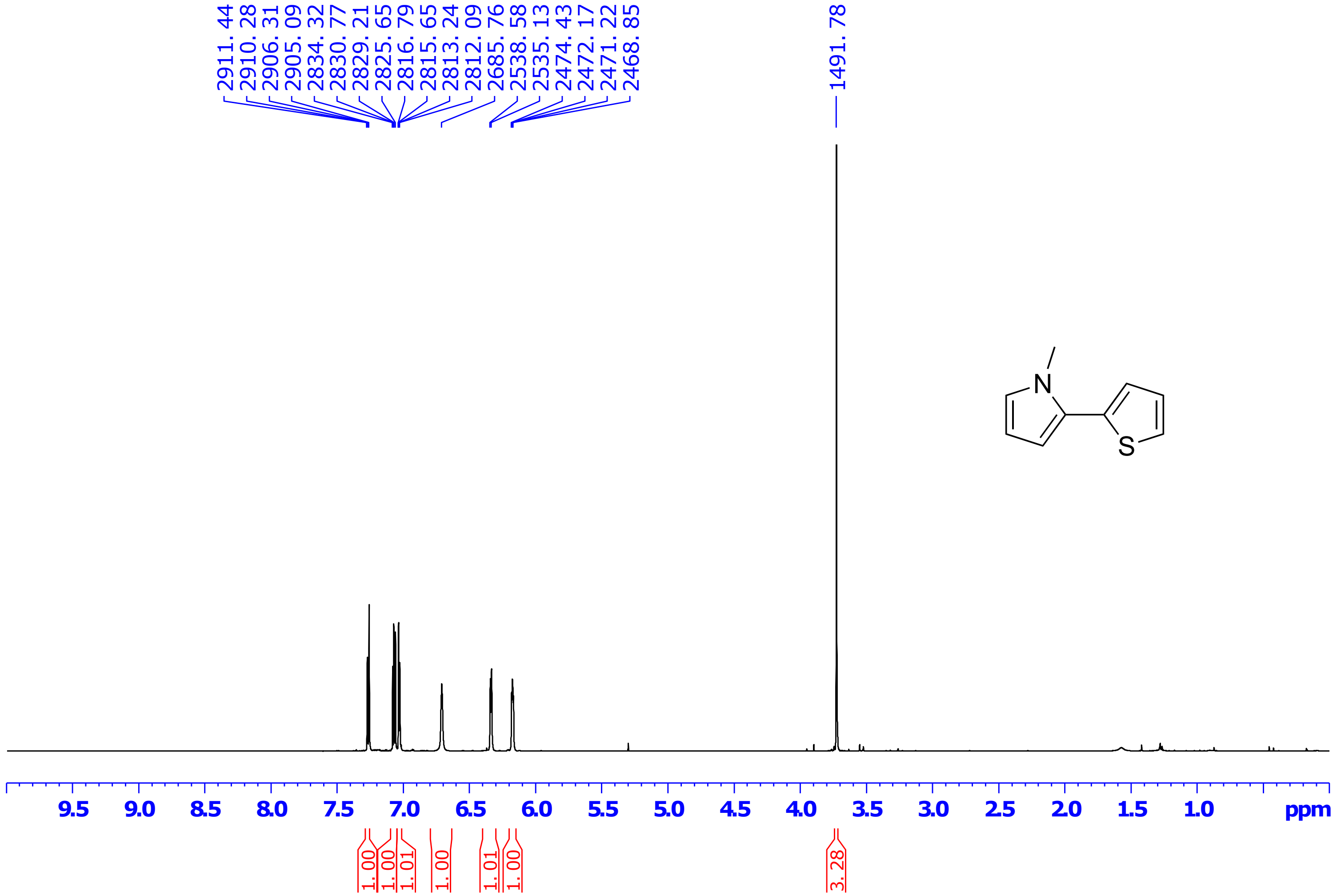

Figure S32 ^{1}H NMR of derivative **4** in $CDCl_3$.

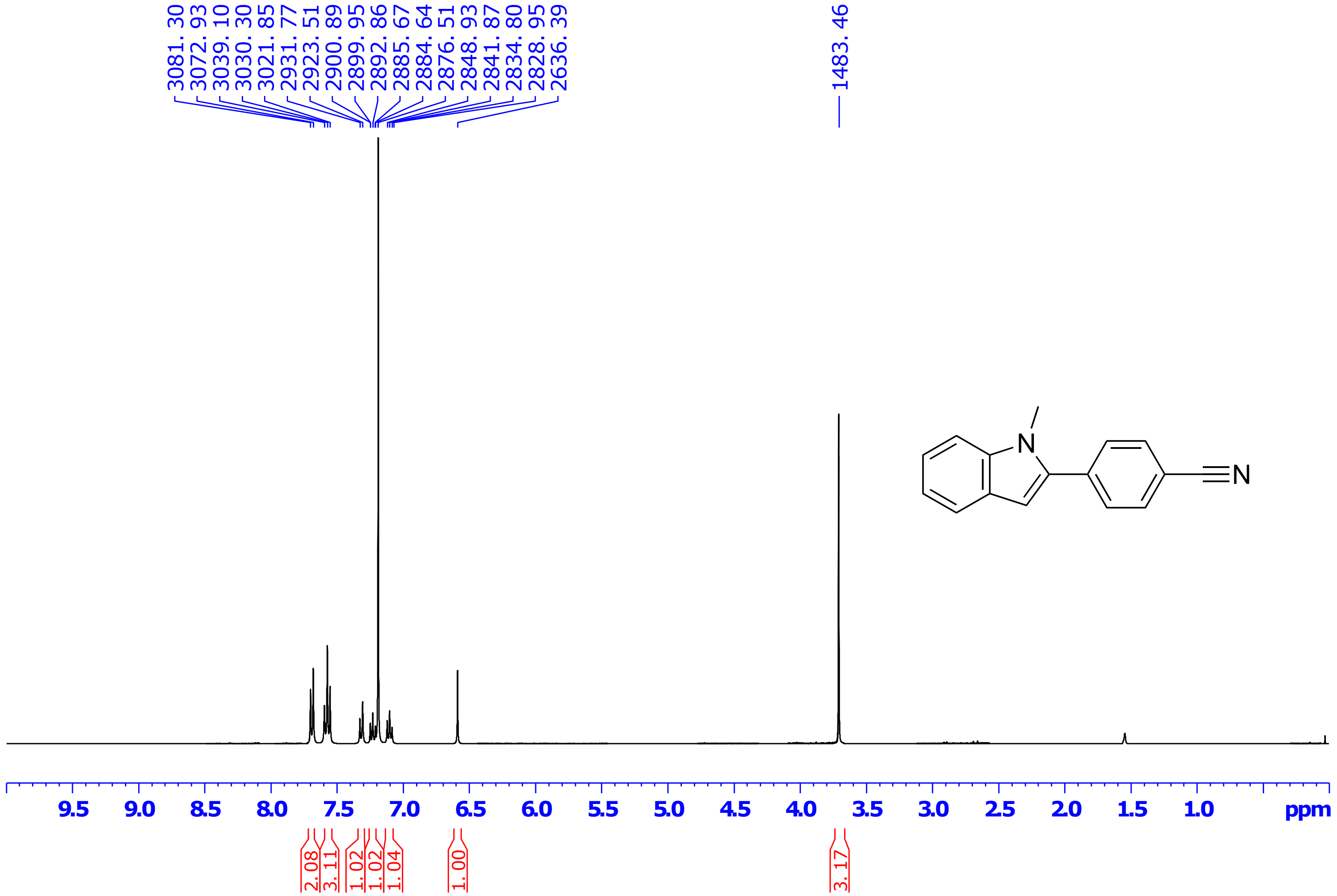

Figure S33 ^{1}H NMR of derivative **7** in $CDCl_3$.

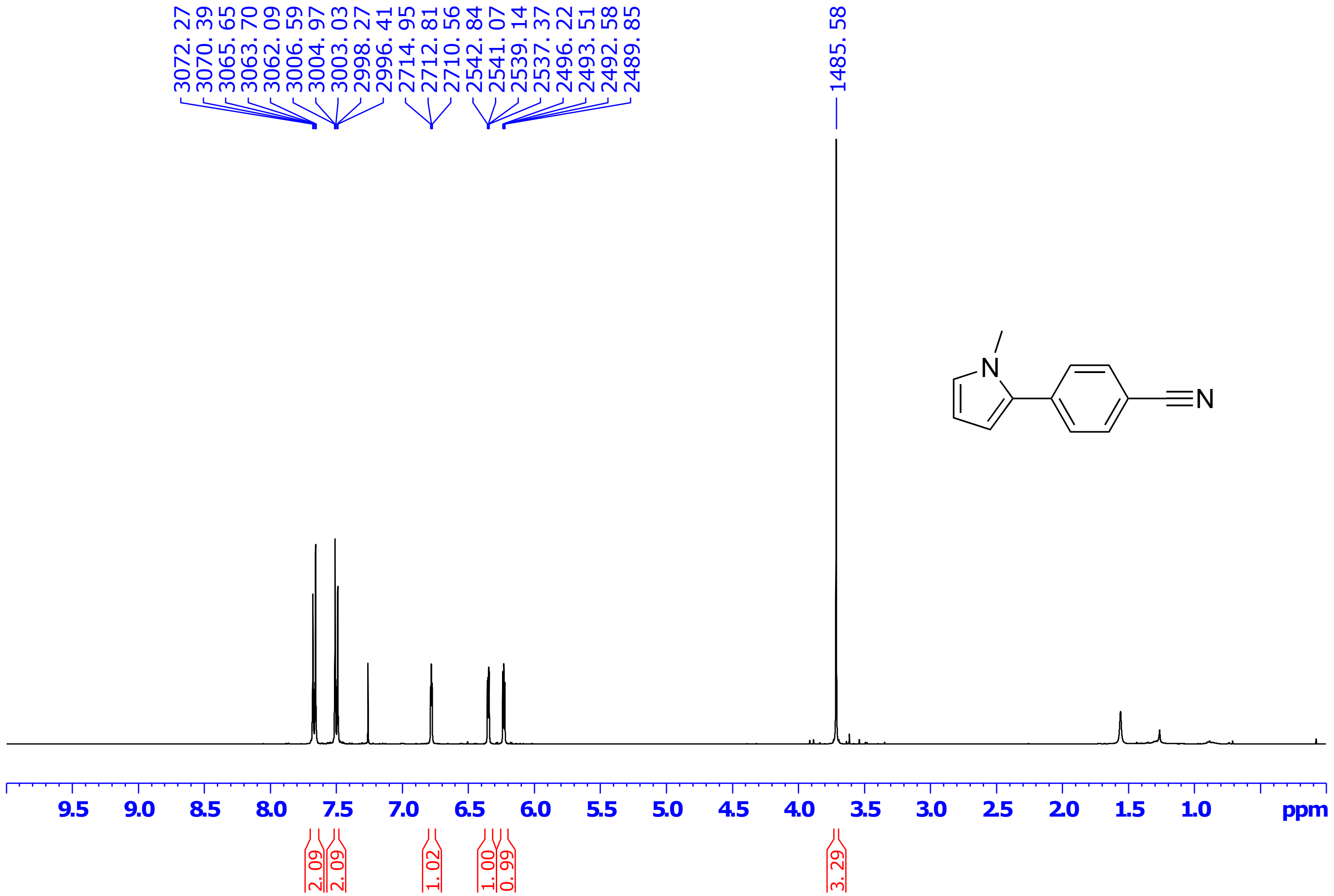

Figure S34 ^{1}H NMR of derivative **8** in $CDCl_3$.

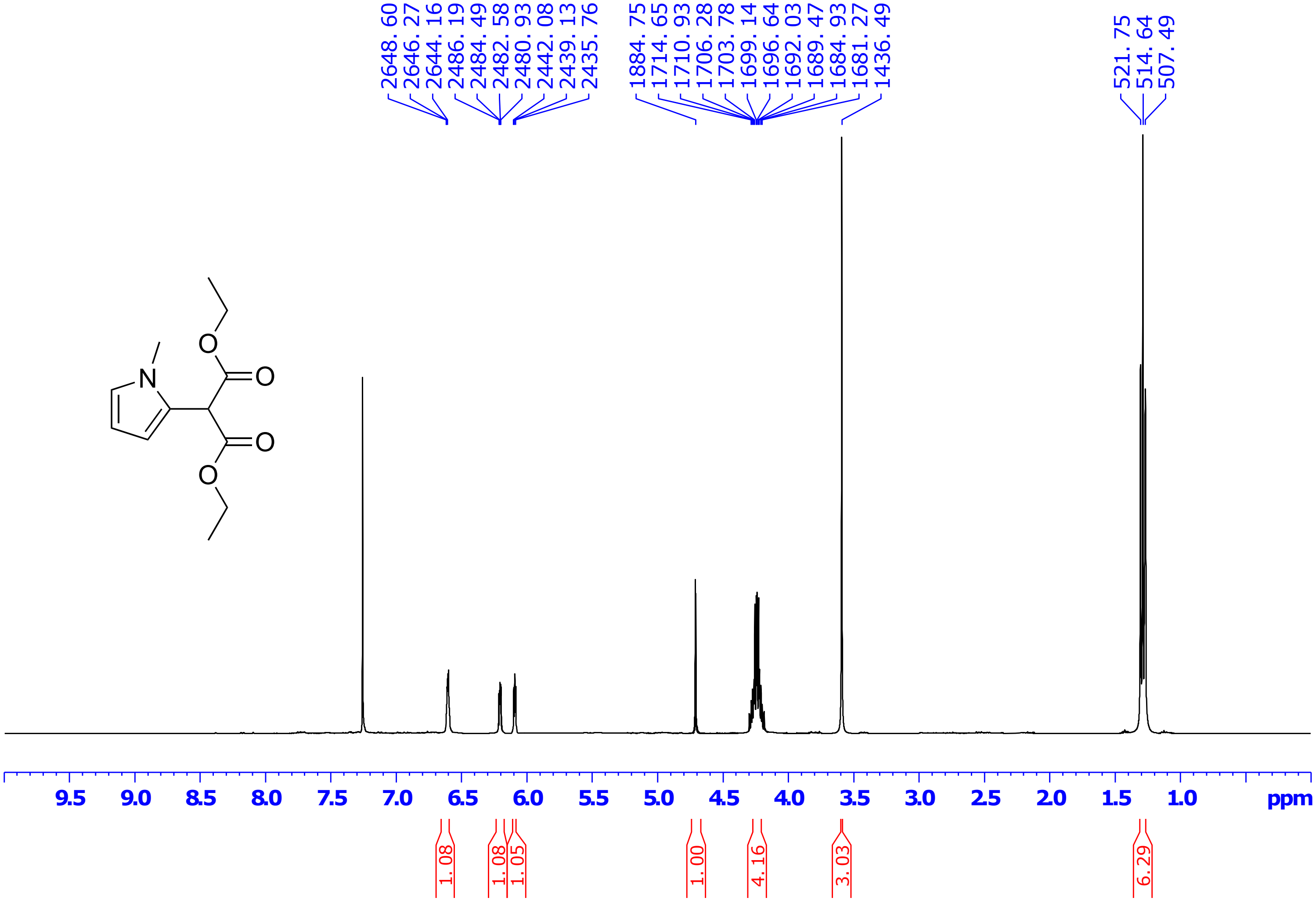

Figure S35 ^{1}H NMR of derivative **9** in $CDCl_3$.

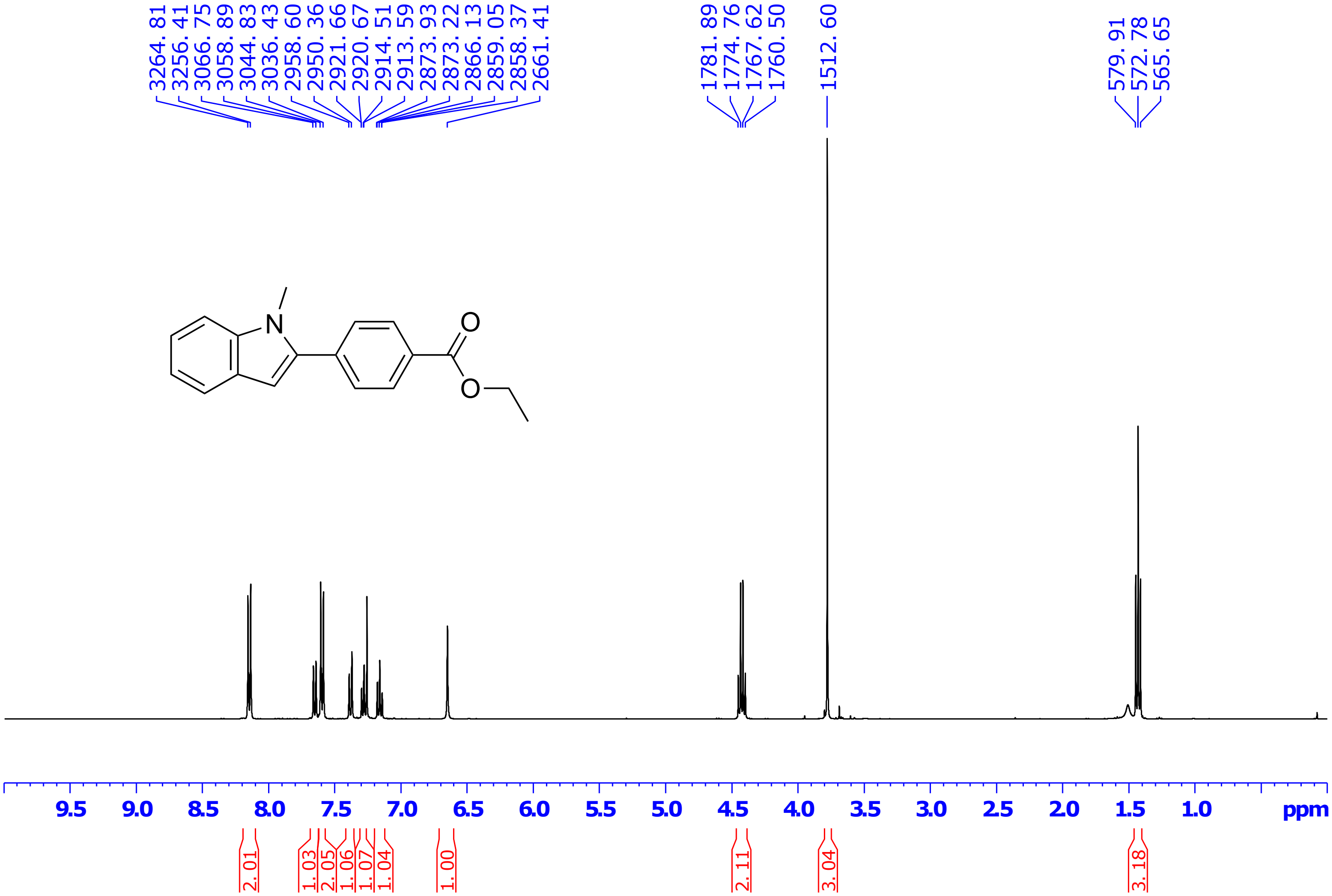

Figure S36 ^{1}H NMR of derivative **10** in $CDCl_3$.

References for the Supporting Information

(S1) Pan, X.; Fang, C.; Fantin, M.; Malhotra, N.; So, W. Y.; Peteanu, L. A.; Isse, A. A.; Gennaro, A.; Liu, P.; Matyjaszewski, K. Mechanism of Photoinduced Metal-Free Atom Transfer Radical Polymerization: Experimental and Computational Studies. *Journal of the American Chemical Society* **2016**, *138*, 2411–2425.

(S2) Mayer, L.; May, L.; Müller, T. J. J. The interplay of conformations and electronic properties in N-aryl phenothiazines. *Organic Chemistry Frontiers* **2020**, *7*, 1206–1217.

(S3) Pavlishchuk, V. V.; Addison, A. W. Conversion constants for redox potentials measured versus different reference electrodes in acetonitrile solutions at 25 °C. *Inorganica Chimica Acta* **2000**, *298*, 97–102.

(S4) Romero, N. A.; Nicewicz, D. A. Organic Photoredox Catalysis. *Chemical Reviews* **2016**, *116*, 10075–10166.

(S5) Discekici, E. H.; Treat, N. J.; Poelma, S. O.; Mattson, K. M.; Hudson, Z. M.; Luo, Y.; Hawker, C. J.; De Alaniz, J. R. A highly reducing metal-free photoredox catalyst: Design and application in radical dehalogenations. *Chemical Communications* **2015**, *51*, 11705–11708.

(S6) Ceriani, C.; Ghiglietti, E.; Sassi, M.; Mattiello, S.; Beverina, L. Taming Troublesome Suzuki-Miyaura Reactions in Water Solution of Surfactants by the Use of Lecithin: A Step beyond the Micellar Model. *Organic Process Research & Development* **2020**, *24*, 2604–2610.

(S7) Horn, C. R.; Gremetz, S. A method to determine the correct photocatalyst concentration for photooxidation reactions conducted in continuous flow reactors. *Beilstein Journal of Organic Chemistry* **2020**, *16*, 871–879.

(S8) Zhang, X.; Smith, N.; Webb, A. In *Biomedical Information Technology*, 2nd ed.; Feng, D. D., Ed.; Biomedical Engineering; Academic Press, 2020; pp 3–49.

(S9) Mollet, H.; Grubenmann, A. *Formulation Technology: emulsions, suspensions, solid forms*; John Wiley & Sons, 2008.